AD-A102 814 GRUMAN AEROSPACE CORP BETHPAGE NY RESEARCH DEPT F/G 20/11
EVALUATION OF STRESS INTENSITY FACTORS IN PRECRACKED OPEN AND R--ETC(U)
APR 81 B P LEFTHERIS, R C SCHWARZ
UNCLASSIFIED RE-628 NL

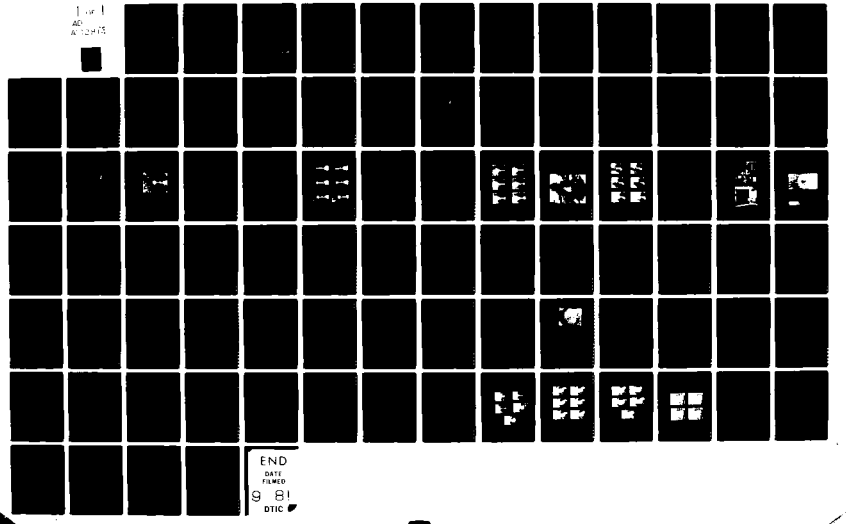

END
DATE FILMED
9 81
DTIC

RE-628

EVALUATION OF STRESS INTENSITY FACTORS IN PRECRACKED OPEN AND RIVETED HOLES USING THE METHOD OF CAUSTICS

By

Basil P. Leftheris *

and

Robert C. Schwarz **

April 1981

Research Department

Grumman Aerospace Corporation

Bethpage, New York 11714

* Senior Staff Scientist, Research Department
** Senior Engineer, Structural Test Engineering Department

UNCLASSIFIED

SECURITY CLASSIFICATION OF THIS PAGE *(When Data Entered)*

REPORT DOCUMENTATION PAGE		READ INSTRUCTIONS BEFORE COMPLETING FORM
1. REPORT NUMBER RE-628	2. GOVT ACCESSION NO. AD-A102	3. RECIPIENT'S CATALOG NUMBER 814
4. TITLE *(and Subtitle)* Evaluation of Stress Intensity Factors in Precracked Open and Riveted Holes Using the Method of Caustics		5. TYPE OF REPORT & PERIOD COVERED
		6. PERFORMING ORG. REPORT NUMBER RE-628
7. AUTHOR(s) Basil P. Leftheris Robert C. Schwarz		8. CONTRACT OR GRANT NUMBER(s)
9. PERFORMING ORGANIZATION NAME AND ADDRESS Grumman Aerospace Corporation Research Department A08/35 Bethpage, New York 11714		10. PROGRAM ELEMENT, PROJECT, TASK AREA & WORK UNIT NUMBERS
11. CONTROLLING OFFICE NAME AND ADDRESS		12. REPORT DATE April 1981
		13. NUMBER OF PAGES 88
14. MONITORING AGENCY NAME & ADDRESS*(if different from Controlling Office)*		15. SECURITY CLASS. *(of this report)* UNCLASSIFIED
		15a. DECLASSIFICATION/DOWNGRADING SCHEDULE

16. DISTRIBUTION STATEMENT *(of this Report)*

Approved for Public Release; Distribution Unlimited

17. DISTRIBUTION STATEMENT *(of the abstract entered in Block 20, if different from Report)*

18. SUPPLEMENTARY NOTES

19. KEY WORDS *(Continue on reverse side if necessary and identify by block number)*

Stress Intensity, Caustics, Fatigue Life, Riveting, Residual Stresses

20. ABSTRACT *(Continue on reverse side if necessary and identify by block number)*

The method of "caustics" is investigated and analyzed as a means of evaluating stress intensity factors, K_I, in cracks radially emanating from holes drilled in aluminum and steel specimens. The results from cracks in open holes in specimens under uniaxial tension loads, are compared with results obtained analytically. Effects of compressive residual stresses in reducing K_I are demonstrated.

DD FORM 1 JAN 73 1473 EDITION OF 1 NOV 65 IS OBSOLETE
S/N 0102-014-6601

UNCLASSIFIED

SECURITY CLASSIFICATION OF THIS PAGE *(When Data Entered)*

Grumman Research Department Report RE-628

EVALUATION OF STRESS INTENSITY FACTORS IN PRECRACKED OPEN AND RIVETED HOLES USING THE METHODS OF CAUSTICS

by

Basil P. Leftheris
Research Department

and

Robert C. Schwarz
Structural Test Engineering Department

April 1981

Approved by:

Richard A. Scheuing
Director of Research

ACKNOWLEDGMENT

The method of caustics was first developed at the Technical University of Athens, Greece under the leadership of Professor Pericles Theocaris. The plethora of publications under his authorship in American and European technical journals attest to his efforts in perfecting the caustics technique.

The authors are grateful to Professor Theocaris for his initial tutelage, continuous support and advice, and his invitation to the first author to his well-equipped laboratory for a first-hand demonstration of caustics. The authors also wish to thank Professor Emmanuel Gdoutos, one of Prof. Theocaris's assistants, for many useful discussions during this study.

SUMMARY

The method of "caustics" is investigated and analyzed as a means of evaluating stress intensity factors, K_I, in cracks radially emanating from holes drilled in aluminum and steel specimens. The results from cracks in open holes and in specimens under uniaxial tension loads, are compared with results obtained analytically (as described by Paris and Sih in ASTM 381-Ref 5). Effects of compressive residual stresses in reducing K_I are demonstrated.

The classical analyses of stress concentrations in the vicinity of a crack tip have led to the determination of stress intensity factors that are useful in predicting design allowable stresses in riveted joints. These analytical predictions have now been related to direct measurement of surface deflections by the method of caustics, which employs laser reflection under controlled conditions. The caustic is the trace of the singular reflection zone in the image plane of an experimental apparatus, and its dimensions are a very sensitive measure of surface slopes. This method, originally devised by P.S. Theocaris in 1972, has been successfully employed in a variety of applications. In this report, we present initial results of its application to the investigation of crack propagation under load as it is affected by residual compressive stress distributions created by dynamically installed interference rivets. When compared with analytical prediction and the results of fatigue tests, we hope that eventually it will be possible to define in advance operating domains within which crack growth will not occur.

Several clear advantages were offered by the method of caustics. For example, classical analytical models imply that $K_I = 0$ when the load is zero. Yet we know that in any crack the residual stress field at the tip will always mean that $K_I \neq 0$. Since the method of caustics

shows large changes in light reflection from small surface deformations near the tip of the crack, it measures K_I accurately enough to determine K_I at no load. Another advantage the caustic gives is the determination of the load at which plastic deformation begins. Again, current analytical models cannot predict such loads, but the sudden enlargement of the caustic is a very good indication of incipient plastic deformation.

Finally, the holes in aluminum and steel specimens were cold worked using a dynamically expanding rivet. We observed that whenever the radius at which the elastic-plastic boundary was expanded beyond the crack, the caustic disappeared; but, if the elastic-plastic radius was smaller than the crack, the caustic increased in size. We believe that the method of caustics can be used with great advantage to evaluate the effectiveness of cold-worked holes in riveted joints.

TABLE OF CONTENTS

LIST OF ILLUSTRATIONS

LIST OF ILLUSTRATIONS (contd)

LIST OF ILLUSTRATIONS (contd)

1. INTRODUCTION

Damage tolerance criteria have been used in recent years to evaluate the economic life of aircraft structures. The current MIL-A-83444 Damage Tolerance Specification requires such criteria to be used in design. They are based on the premise that the structures can withstand the existence of small cracks without catastrophic failures, for the duration of their predicted fatigue life. There are many critical parts in aircraft structures for which premature failure can cause the withdrawal of the aircraft from service because the cost of its repair will exceed the cost of a new aircraft. This limit, called the economic life of the aircraft, is one of the design criteria used to minimize total life cycle costs. One of the most common sources of such failures in aircraft is in the riveted joints. Recently, (Ref 1), we showed that considerable fatigue life enhancement, as well as good economic life and lower initial cost, can be achieved if the joints are riveted with residual compressive stresses. Any evaluation of riveting methods, however, that provides these advantages, involves the evaluation of the stress intensity factors, and the residual stress field from which we can evaluate the remaining fatigue life of damaged (cracked) structures. We have used the new riveting method called Stress Wave Riveter (SWR) (Ref 2) to achieve a considerable degree of fatigue life enchancement in such damaged joints.

An experimental method of evaluating stress intensity factors (K_I) is necessary to provide us with the means to evaluate the degree of enhancement due to a particular residual stress distribution and flaw size quickly and accurately (refer to Appendix A). We selected the method of caustics to explore the feasibility of measuring K_I. Theocaris (Refs 3 and 4) has done considerable work on the theory and applications of caustics. A detailed analysis of caustics is given in Section 2. To illustrate how the method of caustics works, we analyzed a one-dimensional model of a crack

emanating from a hole, and, by using the principles of reflecting rays, we were able to show how the coalescing of light rays form caustics.

We are using a laser beam as an intense collimated monochromatic light source. From an optical point of view unfinished metal surfaces are not good reflectors. To produce good caustics, therefore, we must make every possible effort to obtain smooth surfaces, especially by polishing the specimens. Caustics can be used in many applications. We are interested here only in their application to cracks. In particular, we are using caustics as a non-destructive means of evaluating riveted aluminum and steel structures. In our efforts to improve fatigue life, and to reduce the cost of manufacturing and maintaining aircraft, we feel that diagnostics such as the method of caustics to detect and evaluate cracks will eventually prove to be practical.

Our work consists of making fatigue specimens with holes. Using cyclic loads, we precrack each hole to a specified length. The specimens are polished prior to cracking in accordance with standard metallurgical procedures. The caustics for each cracked hole are then measured and the K_I factors evaluated at various tension loads.

Using the SWR method, rivets are then installed with various degrees of compressive residual stresses (cold work). The K_I values are measured again at various tension loads. Details of the laboratory set-up, test results and evaluation are given in the following sections of this report. The results show clearly that there are regimes of crack length, load and residual stress levels in which stress intensity factors are reduced, and in some cases, eliminated completely.

2. THEORETICAL BACKGROUND

THEORETICAL EXPLANATION OF THE METHOD OF CAUSTICS FOR MEASURING K_I

The derivations of this section follow the methods described by P.S. Theocaris and his colleagues (Ref 3). We have, however, developed the uniaxial case and derived the "ray reflection" method to elucidate the particular case of caustic application to cracks.

The surface deformation around the tip of the crack is given by Eq. (A-4) from the Appendix

$$\Phi(\zeta) = \frac{K^*}{2(2\pi\zeta)^{1/2}} \tag{1}$$

where K^* is the complex stress intensity factor and $\zeta = x + iy$.

Considering a cross section, in the direction of the crack, with only one mode of crack opening, Eq (1) is reduced to

$$\Phi(Z) = \frac{K_I}{2(2\pi x)^{1/2}} \tag{2}$$

The surface deformation, on the other hand, is given by

$$Z = \Delta t = -\frac{\nu t}{2E}(\sigma_1 + \sigma_2) \tag{3}$$

where ν = Poisson's ratio
E = Young's modulus
t = thickness
and σ_1 & σ_2 are the principal stresses around the crack. Paris and Sih, (Ref 5), however, related Eq (2) & (3) by the following:

$$\sigma_1 + \sigma_2 = 4\Phi(Z)$$

Therefore

$$Z = -\frac{\nu t K_I}{E(2\pi x)^{1/2}} \tag{4}$$

Let $$C = \frac{\nu t K_I}{E(2\pi)^{1/2}} \tag{5}$$

Thus $$Z = -\frac{C}{x^{1/2}} \tag{6}$$

Differentiating (6) we obtain

$$\frac{dZ}{dx} = \frac{1}{2}\frac{C}{x^{3/2}} \tag{7}$$

and

$$\frac{d^2Z}{dx^2} = -\frac{3}{4}\frac{C}{x^{5/2}} \tag{8}$$

The geometrical representation of caustics is shown in Fig. 2-1.

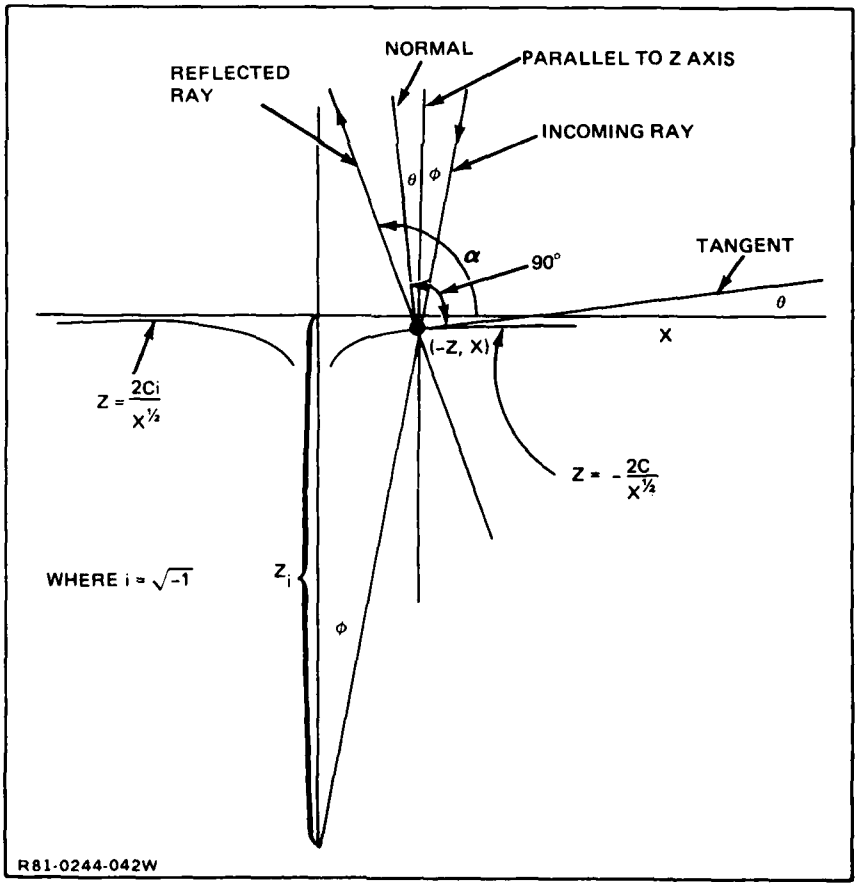

Fig. 2-1 Reflection of Incoming Ray from Surface Adjacent to Crack

The angle of the reflected ray is given by

$$\alpha = 90 + 2\theta + \varphi \ . \tag{9}$$

But,

$$\theta = \tan^{-1} \frac{dZ}{dt} = \tan^{-1} \frac{C}{2x^{3/2}}$$

and

$$\varphi = \tan^{-1} \frac{x}{Z_i} \ .$$

Thus,

$$\alpha = 90 + 2\tan^{-1} \frac{C}{2x^{3/2}} + \tan^{-1} \frac{x}{Z_i} \tag{10}$$

To illustrate the meaning of Eq (10), let us consider a case of an aluminum specimen, 0.125 in. thick, with $K_I = 5 \times 10^3$ psi$\sqrt{\text{in.}}$

Hence $\nu = 0.33$

$E = 10^7$ psi

$t = 0.125$ in.

Substituting in Eq (5) we obtain

$$C = 0.8228 \times 10^{-5}$$

Therefore, using Eq (10) we find the following:

x	α
0.011	90.7238
0.013	90.6905
0.014	90.6856
0.01435	90.6853
0.0145	90.685
0.015	90.688
0.016	90.691
0.017	90.700
0.02	90.740

From a close look at the change of α with x, we see that between $x = 0.014$ and $x = 0.015$, $\Delta\alpha$ changes from negative to positive. In fact,

the point where this change takes place is located at

$$3\theta = \varphi.$$

Since the angles θ and ϕ are very small, we have

$$3\left(\frac{C}{2x^{3/2}}\right) = \frac{x}{Z_i}$$

from which we obtain

$$\frac{3}{2}\,\frac{C}{x^{5/2}} = \frac{1}{Z_i}\ . \tag{11}$$

Comparing Eq (8) with Eq (11) we see that $\Delta\alpha$ changes sign at

$$\frac{d^2Z}{dx^2} = -\frac{1}{2Z_i}\ . \tag{12}$$

Solving Eq (11) for x

we have

$$x_i \simeq \left(\frac{3}{2}\,CZ_i\right)^{2/5}\ . \tag{13}$$

where x_i is the innermost point inside of which reflected rays diverge. For the numerical case we considered above we have

$$x_i = 0.01435 \text{ in.}$$

or, an angle $\theta = 0.1371°$ and $\alpha = 90.6853$.

If we now place a screen at a distance Z_0 from the specimen we have the geometry shown in Fig. 2-2.

Considering the triangle ABC, in Fig. 2-2, we have

$$w = x - (Z_0 + Z)\tan(2\theta + \varphi) \tag{13}$$

or

$$w = x - (Z_0 + Z)\,\frac{\tan 2\theta + \tan\varphi}{1 - \tan 2\theta \tan\varphi}\ .$$

Since θ and φ are small angles, we set $\tan 2\theta = 2\tan\theta = 2(dZ/dx)$ and $\tan 2\theta \tan\varphi \cong 2\tan\theta \tan\varphi \cong 0$; $\tan\varphi = x/Z_i$.

From our previous discussion we know that below the value x_i (for example $x_i = 0.01435$ in.) reflected rays will diverge. These rays do

not contribute to the caustic formation. The value of x_i is given by Eq (13). For $x > x_i$, however, reflected rays converge. The condition of convergence of two or more rays, at the O'x' axis on the screen, is expressed by setting the Jacobian equal to zero. In our one dimensional model this condition is given by

$$\frac{dw}{dx} = 0 .$$

Differentiating Eq (13) we obtain:

$$\frac{dw}{dx} = 1 - 2Z_0 \frac{d^2Z}{dx^2} - \frac{Z_0}{Z_i} = 0 .$$

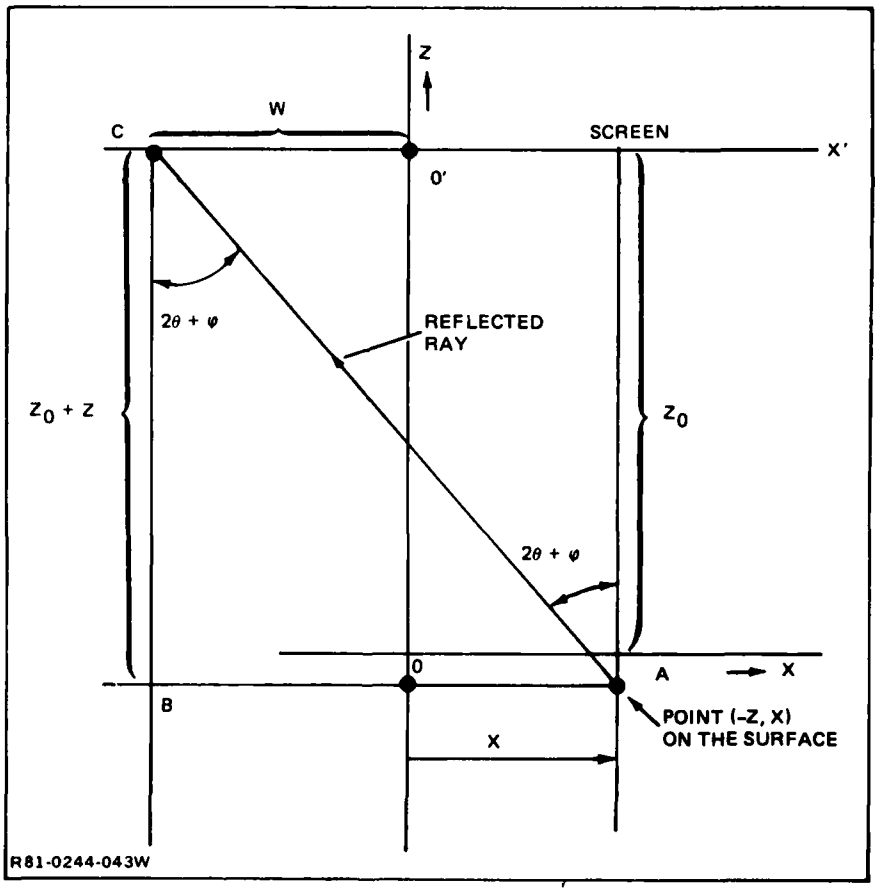

Fig. 2-2 Geometry with Screen, where Caustic is Formed

Hence $$-1+\frac{Z_0}{Z_i}=-2Z_0\frac{d^2Z}{dx^2}$$

and $$\frac{Z_0}{Z_i}-1=-2Z_0\frac{d^2Z}{dx^2}\quad . \tag{14}$$

The ratio $\frac{Zo+Zi}{Zi}=\lambda_m$ represents the amplification factor of a converging laser beam (Note $Z_i < 0$). Hence,

$$\frac{2Z_0}{\lambda_m}\frac{d^2Z}{dx^2}=-1\ .$$

Substituting from Eq (8) we have

$$\frac{3}{4}\frac{C}{x_i^{5/2}}=\frac{\lambda_m}{2Z_0}$$

and $$x_i^{5/2}=\frac{3CZ_0}{2\lambda_m} \tag{15}$$

and $$x'=r_0=\left\{\frac{3\nu tZ_0K_r}{2E(2\pi)^{1/2}}\lambda_m\right\}^{2/5}\quad . \tag{16}$$

Thus, the point where two converging rays meet in the O'x' axes is given by

$$x'=\left(\frac{3C\,Z_0}{2\lambda_m}\right)^{2/5} \tag{17}$$

Rearranging Eq (13) we have:

$$w=x-2Z_0\frac{dZ}{dx}-Z_0\tan\varphi\ ,$$

and

$$w=x-Z_0\frac{C}{x^{3/2}}-\frac{Z_0x}{Z_i}$$

$$=x-\frac{Z_0C}{x^{3/2}}-\frac{Z_0x}{Z_i}\ , \tag{18}$$

or $$w=x-\frac{Z_0Cx}{x^{5/2}}-\frac{Z_0x}{Z_i}\quad . \tag{19}$$

Substituting from Eq (15) we have

$$w = -x\left(\frac{Z_0 - Z_i}{Z_i}\right) - \frac{Z_0 C x}{x^{5/2}} = -\lambda_m x\left\{1 + \frac{Z_0 C}{\lambda_m x^{5/2}}\right\} \qquad (20)$$

or

$$w = -\lambda_m x\left[1 \pm \frac{2}{3}\right], \qquad (21)$$

and finally, $w = 5/3(\lambda_m x_i)$ (i.e., maximum) and $w = 1/3\ \lambda_m x_i$ (i.e., minimum.) Thus, from Eq (15) we have:

$$K_I = \frac{2E(2\pi)^{1/2}}{3\nu t Z_0 \lambda_m} r_0^{5/2} = \frac{2E(2\pi)^{1/2}}{\lambda_m^{3/2} 3\nu t Z_0}\left(\frac{D}{\delta}\right)^{5/2} \qquad (22)$$

where D is the diameter of the caustic perpendicular to the crack axis and $D = \delta r_0 \lambda_m$. The caustic formation can be shown graphically (see Fig. 2-3).

To evaluate D, it is necessary to carry out the two dimensional case (Ref 3). For this purpose, consider a specimen with a hole from which a crack is growing (see sketch below).

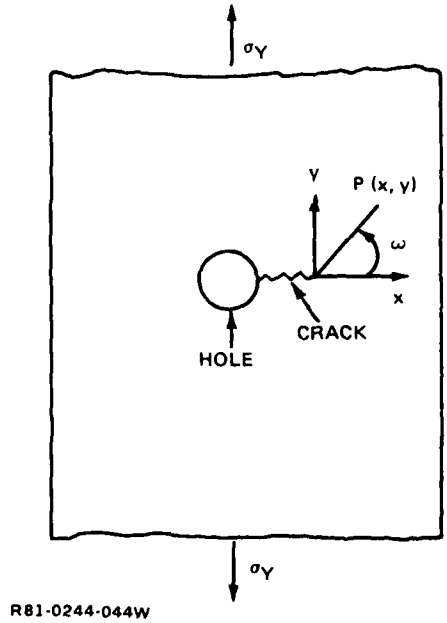

R81-0244-044W

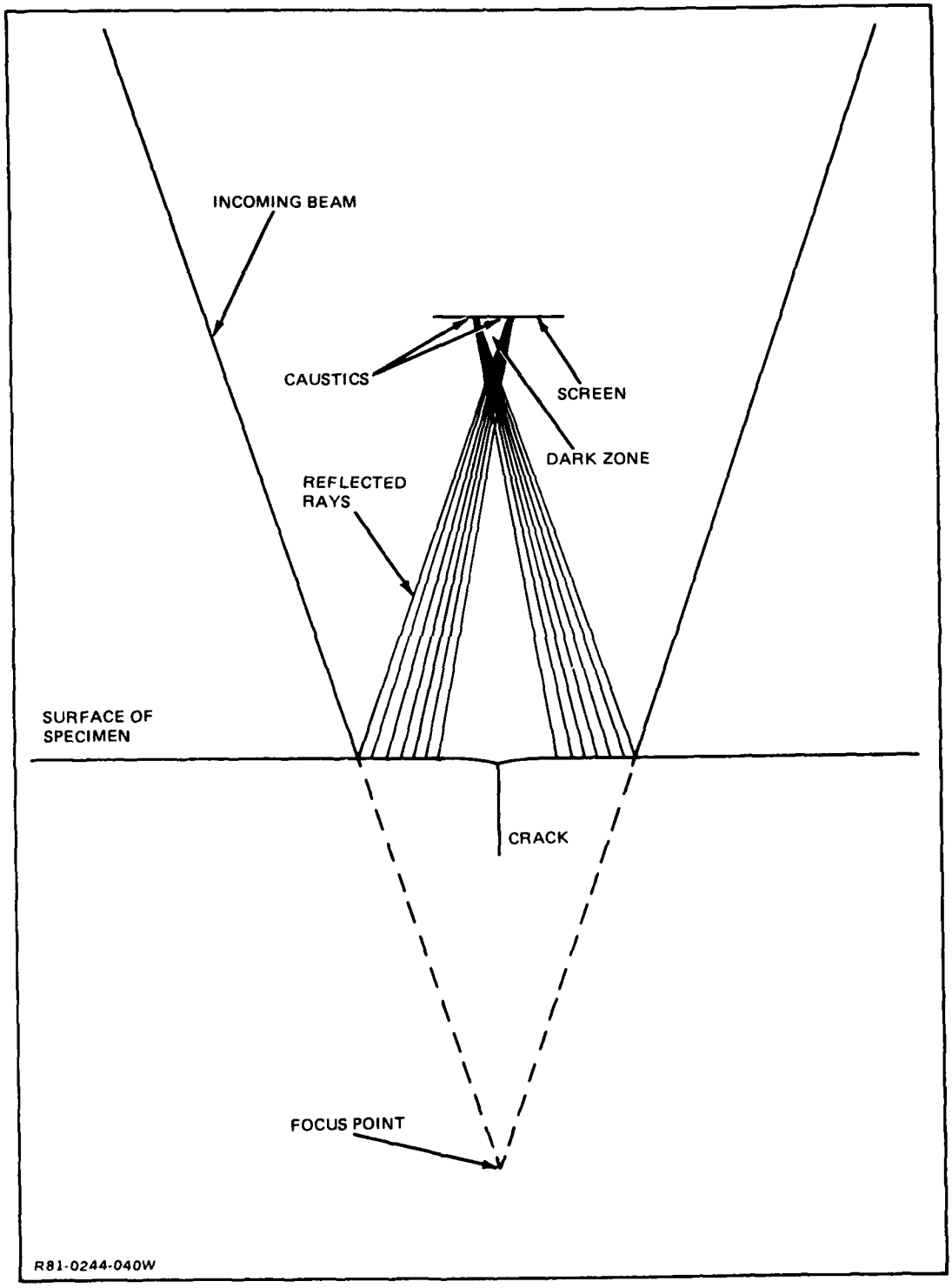

Fig. 2-3 Optical Formation of Caustics

At a point P the deflection due to the crack is given by

$$\Phi(\zeta) = \frac{K_I}{2(2\pi\zeta)^{1/2}} = \frac{K_I e^{-i(\omega/2)}}{2(2\pi r)^{1/2}} \tag{23}$$

where

$$\zeta = x + iy = re^{i\omega}$$

The half distance w of the caustic from the screen, placed Z_0 distance away is given by: $w = \zeta - (Z_0 + Z)\tan(2\theta + \varphi)$. This equation can be further reduced to,

$$w = \zeta - 2Z_0 \tan\theta - Z_0 \tan\varphi;$$

using Eqs (3) & (4) we obtain

$$w = \zeta + Z_0 \frac{\nu t}{E} \text{ grad}[4\,\text{Re}\Phi(\zeta)] - \frac{Z_0\zeta}{Z_i} \tag{25}$$

From Eq (13) we derive the $\text{Re}\Phi(\zeta)$ to be,

$$u(r, w) = \frac{K_I \cos\frac{\omega}{2}}{2(2\pi r)^{1/2}} \tag{26}$$

The grad $u = (\partial u/\partial r) + i(1/r)(\partial u/\partial\theta)$, since $\Phi(\zeta)$ is a harmonic function. Hence,

$$\text{grad}\, u = \frac{K_I}{2(2\pi)^{1/2}} \left\{ -\frac{\cos\frac{\omega}{2}}{2r^{3/2}} - \frac{i\sin\frac{\omega}{2}}{2r^{3/2}} \right\} = -\frac{K_I\left\{\cos\frac{\omega}{2} + i\sin\frac{\omega}{2}\right\}}{4(2\pi)^{1/2}\, r^{3/2}} \tag{27}$$

Substituting Eq (27) into Eq (25) we obtain

$$w = x' + iy' = -re^{i\omega}\left(\frac{Z_0 - Z_i}{Z_i}\right) + \frac{Z_0 \nu t K_I e^{-i(\omega/2)}}{E(2\pi)^{1/2} r^{3/2}}$$

or

$$x' + iy' = re^{i\omega}\lambda_m \left\{ -1 + \frac{Z_0 \nu t K_I e^{-i5\omega/2}}{E(2\pi)^{1/2} r^{5/2}} \right\} \tag{28}$$

where

$$\lambda_m = \frac{Z_0 - Z_i}{Z_i} \quad .$$

Considering now the (x, y) coordinates where $\zeta = x + iy$, and (x', y') coordinates of the screen, we know that <u>there is not one to one correspondence,</u> since distinct points on the Z(x, y) converge into a single point in the (x', y') plane. This statement is expressed by

the Jacobian J = 0

or

$$J = \frac{\partial(\omega_x, \omega_y)}{\partial(x, y)} = \begin{vmatrix} \frac{\partial \omega_x}{\partial x} & \frac{\partial \omega_x}{\partial y} \\ \frac{\partial \omega_y}{\partial x} & \frac{\partial \omega_y}{\partial y} \end{vmatrix} = 0 \qquad (29)$$

where,

$$\left.\begin{aligned} \omega_x &= \lambda_m x - 2Z_0 \frac{\partial f}{\partial x} \\ \omega_y &= \lambda_m y - 2Z_0 \frac{\partial f}{\partial y} \end{aligned}\right\} \qquad (30)$$

and $f(x, y) = -(4\nu t/2E)\mathrm{Re}\Phi(\zeta)$ represents the surface deformation due to the crack formation.

Differentiating each of the Eq (30), substituting into (29) and evaluating the determinant we obtain the following:

$$\left(\lambda_m - 2Z_0 \frac{\partial^2 f}{\partial y^2}\right)\left(\lambda_m - 2Z_0 \frac{\partial^2 f}{\partial y^2}\right) - 4Z_0^2 \left(\frac{\partial^2 f}{\partial x \partial y}\right)^2 = 0$$

or

$$\lambda_m^2 - 2Z_0\lambda_m\left(\frac{\partial^2 f}{\partial y^2} + \frac{\partial^2 f}{\partial x^2}\right) + 4Z_0^2\left[\left(\frac{\partial^2 f}{\partial x^2}\right)\left(\frac{\partial^2 f}{\partial y^2}\right) - \left(\frac{\partial^2 f}{\partial x \partial y}\right)^2\right] = 0 \qquad (31)$$

The function f, however, can be considered harmonic (Ref 5) and therefore the Cauchy-Rieman relations apply.

Thus, if

$$\left.\begin{aligned} &f(\zeta) = u(x, y) + iv(x, y), \text{ where } \zeta = x + iy, \\ &\text{we have} \quad \frac{\partial u}{\partial x} = \frac{\partial v}{\partial y} \text{ and } \frac{\partial v}{\partial x} = -\frac{\partial u}{\partial y}\ . \end{aligned}\right\} \qquad (32)$$

As suggested by Paris and Sih, however, we need only consider the real part of $f(\zeta)$.

From Eq (32) we can easily prove that $(\partial^2 u/\partial x^2) + (\partial^2 u/\partial y^2) = 0$,

and since $$\frac{\partial^2 f}{\partial \zeta^2} = \frac{\partial^2 u}{\partial x^2} + i\frac{\partial^2 v}{\partial x^2}, \quad \left|\frac{\partial^2 f}{\partial \zeta^2}\right| = \left(\frac{\partial^2 u}{\partial x^2}\right)^2 + \left(\frac{\partial^2 v}{\partial x^2}\right)^2 \qquad (33)$$

Furthermore $\frac{\partial^2 u}{\partial x^2} = -\frac{\partial^2 u}{\partial y^2}$, hence $\left(\frac{\partial^2 u}{\partial x^2}\right)^2 = -\left(\frac{\partial^2 u}{\partial x^2}\right)\left(\frac{\partial^2 u}{\partial y^2}\right)$

and $\left(\frac{\partial^2 v}{\partial x^2}\right)^2 = \left(\frac{\partial^2 u}{\partial x \partial y}\right)^2$. (34)

Substituting Eq (33) and (34) into Eq (31) and

$$\lambda_m^2 - \left(\frac{4\nu t Z_0}{E}\right)^2 \left|\frac{\partial^2 \phi}{\partial \zeta^2}\right|^2 = 0 . \tag{35}$$

From Eq (23) we obtain

$$\frac{\partial^2 \phi}{\partial \zeta^2} = \frac{3}{8} \frac{K_I \zeta^{-5/2}}{(2\pi)^{1/2}}$$

and

$$\left|\frac{\partial^2 \phi}{\partial \zeta^2}\right|^2 = \left\{\frac{3}{8} \frac{K_I r^{-5/2}}{(2\pi)^{1/2}}\right\}^2 \tag{36}$$

Substituting into Eq (35) we have:

$$r_0^{5/2} = \frac{3}{2} \frac{K_I \nu t Z_0}{(2\pi)^{1/2} E \lambda_m} . \tag{37}$$

Equation (37) is valid only at the point where Eq (35) holds true.

Substituting in Eq (28) we have,

$$w = r_0 \lambda_m e^{i\omega} \left(-1 + \frac{2}{3} e^{-i(3\omega/2)}\right) \tag{38}$$

The value of r_0 is equivalent to the value of x_i of Eq (13) in the uniaxial case and it represents the limit that separates the rays that converge from the rays that diverge.

Thus,

$$x' = r_0 \lambda_m \left\{\cos\omega + \frac{2}{3} \cos\frac{3\omega}{2}\right\}$$

and

$$y' = r_0 \lambda_m \left\{\sin\omega + \frac{2}{3} \sin\frac{3\omega}{2}\right\} . \tag{39}$$

At the point where x' is zero we have y' = D/2, while $D = \delta r_0$ along the y' axis. x' = 0 is equivalent to

$$\cos\omega + \frac{2}{3} \cos\frac{3\omega}{2} = 0 .$$

This equation is satisfied in the first quadrant at $\omega = 75°$. Evaluating y' at $\omega = 75°$ we obtain $y' = 1.582\ r_0\lambda_m$. Therefore, $D = 3.164\ r_0\lambda_m$ from which we have $\delta = 3.164$.

Rearranging Eq (22) we obtain:

$$K_I = \frac{1.671\,E}{\nu t Z_0 \lambda_m^{3/2}} \left(\frac{D}{3.164}\right)^{5/2} \tag{40}$$

By measuring D on the screen at a distance Z_0, we obtain the value of K_I.

When we analyzed the uniaxial case at y = 0, we found the interesting relationship expressed by Eq (11) independently of the Jacobian, by observing the values of the angle α. Can Eq (11) apply at any angle, other than $\omega = 0$? Using ζ instead of x in Eq (11) we can easily find the unique solution of $\omega = 0°$. Hence, $3\theta = \phi$ is true at $\omega = 0$ only.

AN ILLUSTRATIVE EXAMPLE OF CAUSTICS

Let us consider a set of coordinates (Z, x) in a plane (see sketch below).

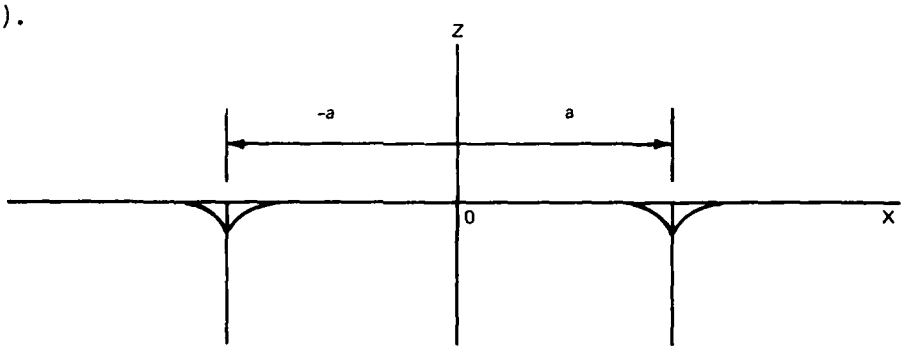

R81-0244-045W

A crack, with its center at x = a can be represented by the following equation.

$$x = a \pm \frac{K^2}{Z^2}\ ,\ \text{where } a > 0 \text{ and } x > 0$$

For a crack with its center at x = - a we have

$$x = -a \pm \frac{K^2}{Z^2}\ ,\ \text{where } a < 0 \text{ and } x < 0\ .$$

In both cases K is a constant to be determined experimentally.

Let us now consider the case of a = - 0.630 in. For the branch x < a, we have,

$$Z = -\frac{K}{(a-x)^{1/2}} \tag{41}$$

and for the branch x > a

$$Z = -\frac{K}{(x-a)^{1/2}} \tag{42}$$

Of course, at x = a, we have a discontinuity, a characteristic of any crack.

Differentiating Eq (41) and (42) we obtain

$$\frac{dZ}{dx} = -\frac{K}{2}\frac{1}{(a-x)^{3/2}}, \quad x<a \tag{43}$$

and

$$\frac{dZ}{dx} = \frac{K}{2}\frac{1}{(x-a)^{3/2}}, \quad x>a\,. \tag{44}$$

Let a converging light beam with a focus at Z_i = - 1.875 in., be directed on the surface that contains the crack along (AB) (see sketch below).

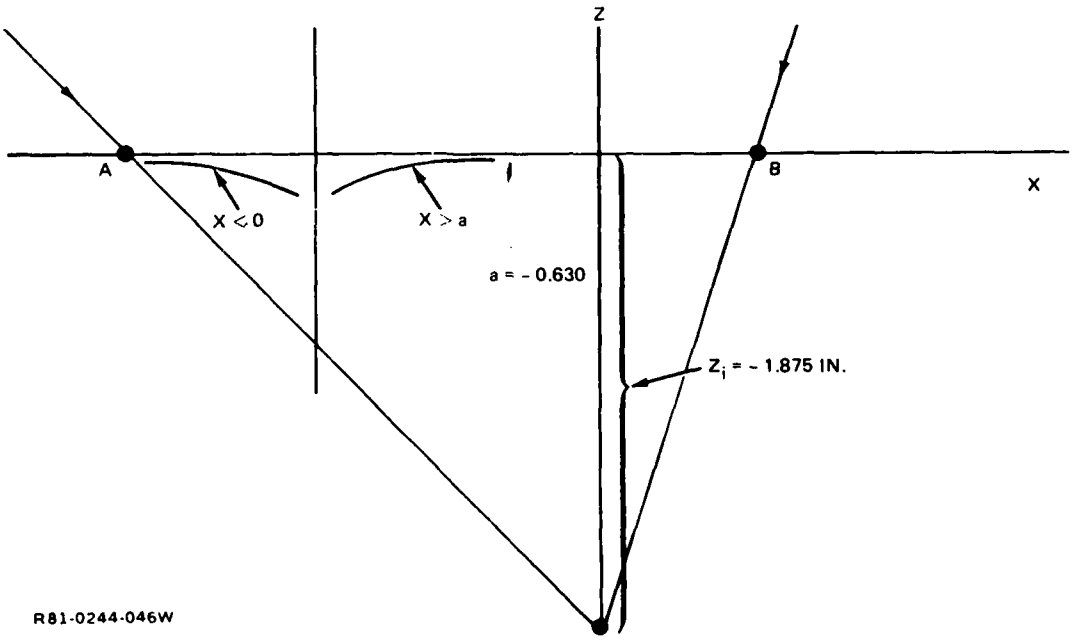

From Eq (44) we have

$$\theta' = \tan^{-1}\left\{ \frac{K}{2} \frac{1}{(x-a)^{3/2}} \right\} \text{ (see Fig. 2-4)} \qquad (45)$$

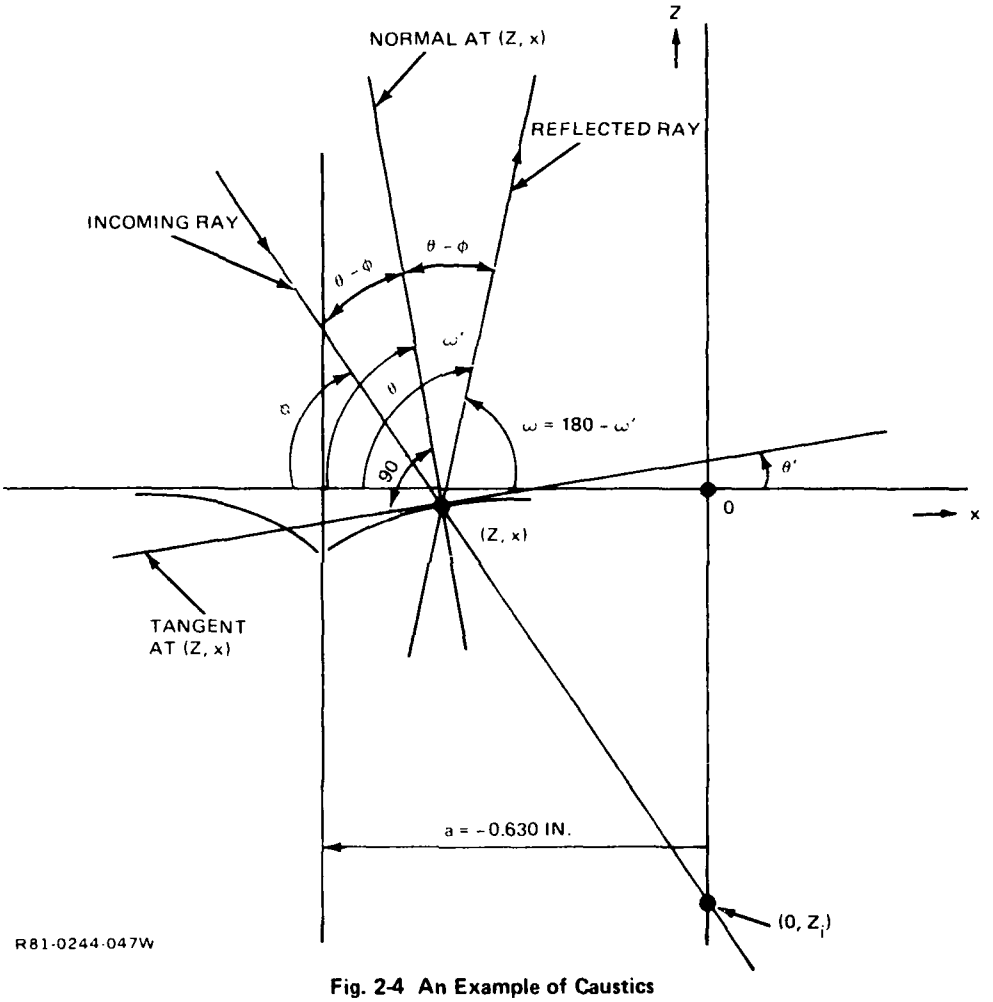

Fig. 2-4 An Example of Caustics

Positive when measured counterclockwise and

$$\theta = -\tan^{-1}\left\{ -\frac{2(x-a)^{3/2}}{K} \right\} \qquad (46)$$

measured clockwise.

The angle $\phi = -\tan^{-1}(Z_i/x)$ measured clockwise.

From the geometry of the diagram we easily deduce that

$$\omega' = 2\theta - \varphi = -2\tan^{-1}\left\{-\frac{2(x-a)^{3/2}}{K}\right\} + \tan^{-1}\left(\frac{Z_i}{x}\right) \quad X \text{ where } Z << Zi;$$

but $\omega = 180 - \omega'$ (ω' is measured clockwise, and ω counterclockwise)

Hence,
$$\omega = 180 - 2\tan^{-1}\left\{\frac{2x-a)^{3/2}}{K}\right\} + \tan^{-1}\left(\frac{Z_i}{x}\right) \qquad (47)$$

when $\omega = 80°$, $Z_i = -1.875$ in., $a = -0.630$ in., and x = -0.50 in.

(These values were measured from a geometric construction of caustics)

Hence,

$$\omega' = 180 - \omega = 100°, \quad \varphi = \tan^{-1}\frac{1.875}{0.50} = 75°$$

and
$$\theta = \frac{\omega' + \varphi}{2} = 87.5° \ .$$

Therefore
$$\tan\theta = \frac{2(x-a)^{3/2}}{K}$$

or
$$K = \frac{2(x-a)^{3/2}}{\tan\theta} = \frac{2(-0.50+0.630)^{1.5}}{\tan 87°} = 0.011$$

and
$$K = 4.91 \times 10^{-3}$$

Thus, the angle ω for various values of x is given by Eq (47) with $K = 4.91 \times 10^{-3}$

$$\omega = 180 - 2\tan^{-1}\{203.64\,(x+0.630)^{1.5}\} + \tan^{-1}\left(\frac{-1.875}{x}\right) \qquad (48)$$

or

for $x > -0.630$

and
$$\omega = -180 + 2\tan^{-1}\{203.64(-(0.63+x))^{1.5}\} + \tan^{-1}\left(\frac{1.875}{x}\right) \qquad (49)$$

for $x < -0.630$

The results are plotted in Fig. 2-5.

x	ω
-0.25	84.8°
-0.50	80°
-1.00	59.43°
-1.125	57.43°
-1.25	55.12°

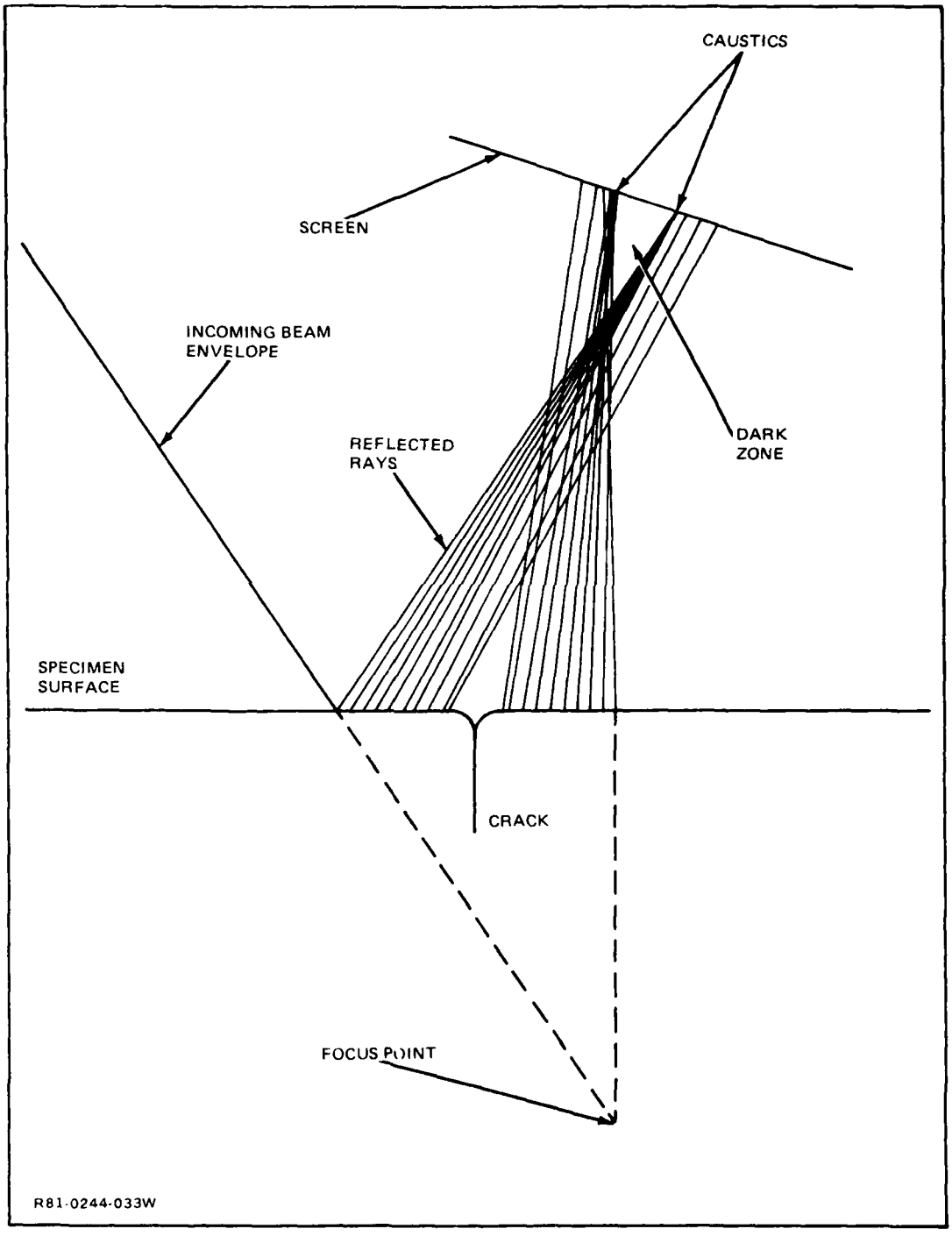

Fig. 2-5 Formation of Caustics

A caustic obtained from a precracked open hole on an aluminum specimen is shown in Fig. 2-6. In this example, the crack is long and we can distinguish the straight portion that is already separated from the circular portion which represents the tip of the crack. In this example, the crack is at the Z axis and

$$Z = \frac{0.8228 \times 10^{-5}}{x^{1/2}}$$

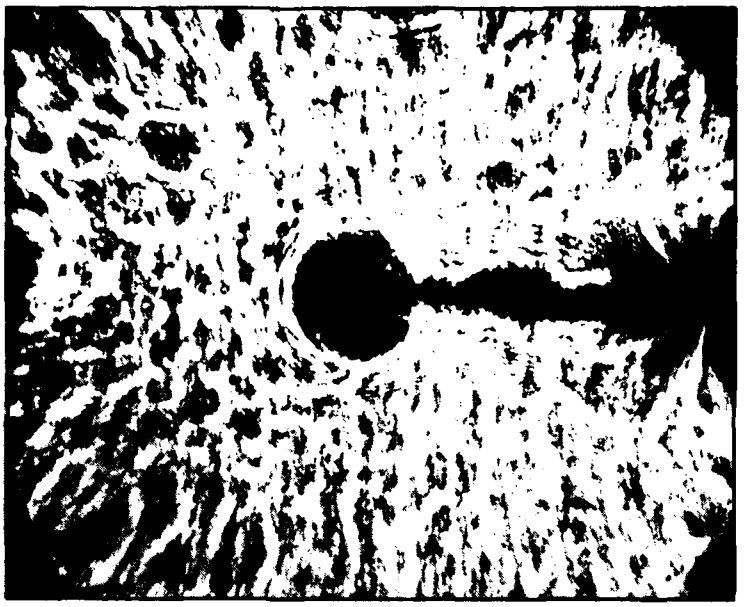

R81-0244-041W

Fig. 2-6 Specimen 3C at 2250 Lbs

It represents the uniaxial case discussed earlier in this section. Information pertaining to the specimen is given in Fig. 2-7. The value of D was measured and K_I was evaluated from Eq (40) for various tension loads σ. The details are given in Section 3. The theoretical estimate of K_I is given by $K_I = k\sigma\sqrt{\pi a}$ where

a = crack length

k = depends on the ratio (a/d), (d = hole diameter)

σ = uniaxial stress on specimen

This equation was taken from ASTM 381 by Paris and Sih (Ref 5).

The caustics of the same crack under various loads are shown in Fig. 2-8. The increase of the large circular area at the tip of the crack with load corresponds to the graph shown in Fig. 2-7.

CRACKS IN HOLES WITH RESIDUAL STRESSES

From work done previously (Ref 1) we know that fatigue life in riveted joints increases, if the fastener generates residual stresses in the radial and circumferential directions. Some fasteners, like Hi-Tique and Taper-Lok, generate radial compressive, but circumferentially tensile stresses. This is accomplished through radial interference by installing a pin with larger diameter than the hole. However, greater increases in fatigue life can be obtained when a radially expanding rivet plastically deforms the material around it, so that upon relaxation of the installation forces, compressive residual stresses are generated in both the radial and circumferential directions. This method of rivet installation is also known as "cold working the hole".

The degree of fatigue life enhancement depends on the extent we cold work the hole, more specifically, how large the radius of the elastic-plastic interface becomes during plastic deformation. The elastic-plastic interface is defined as the radial position (r_p), inside which we have a compressive biaxial field and beyond which the circumferential stresses become tensile (see Fig. 2-9). If a crack emanating from the

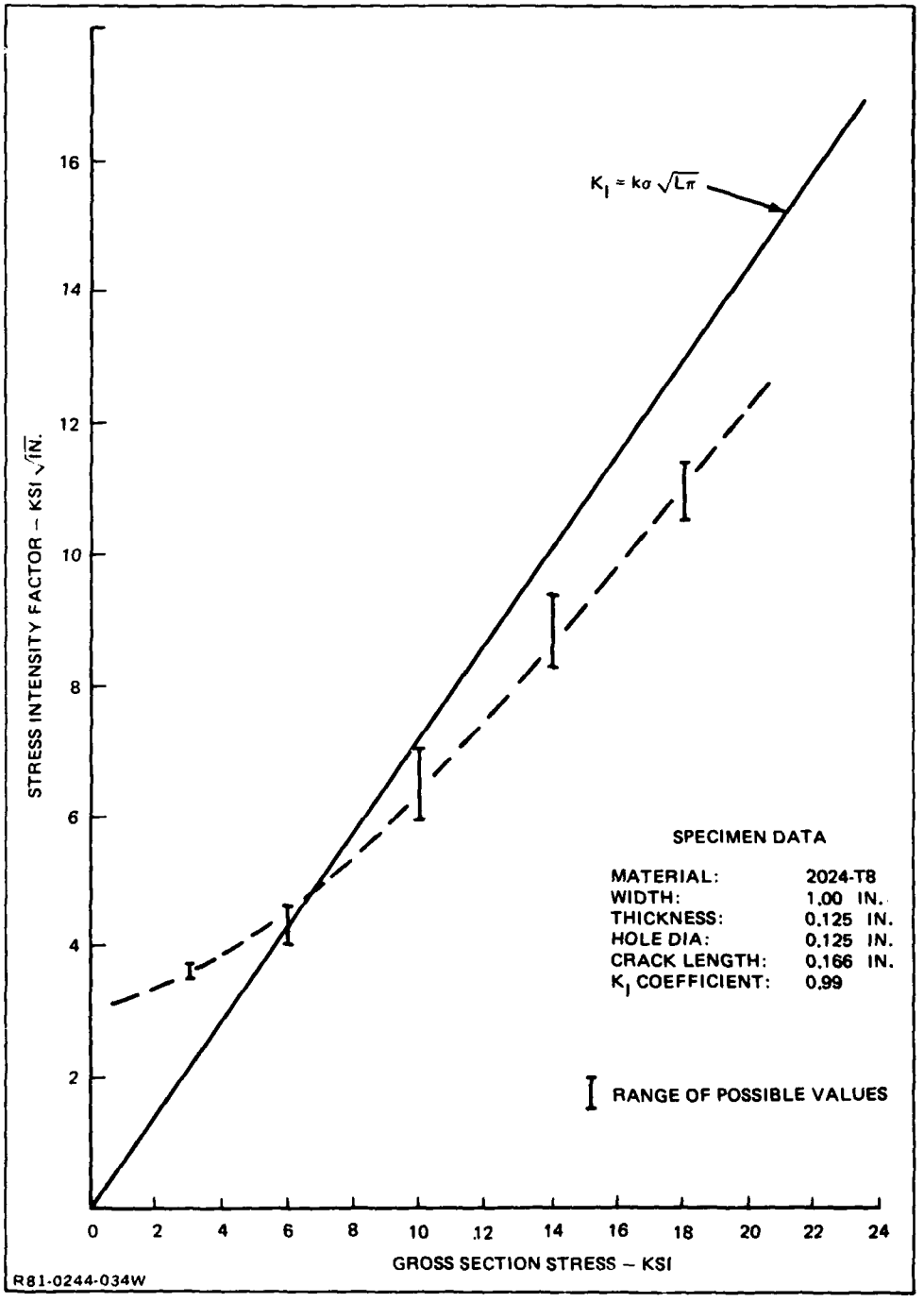

Fig. 2-7 Stress Intensity Factors (ksi $\sqrt{\text{in.}}$), Caustics vs Theory, Specimen 3C

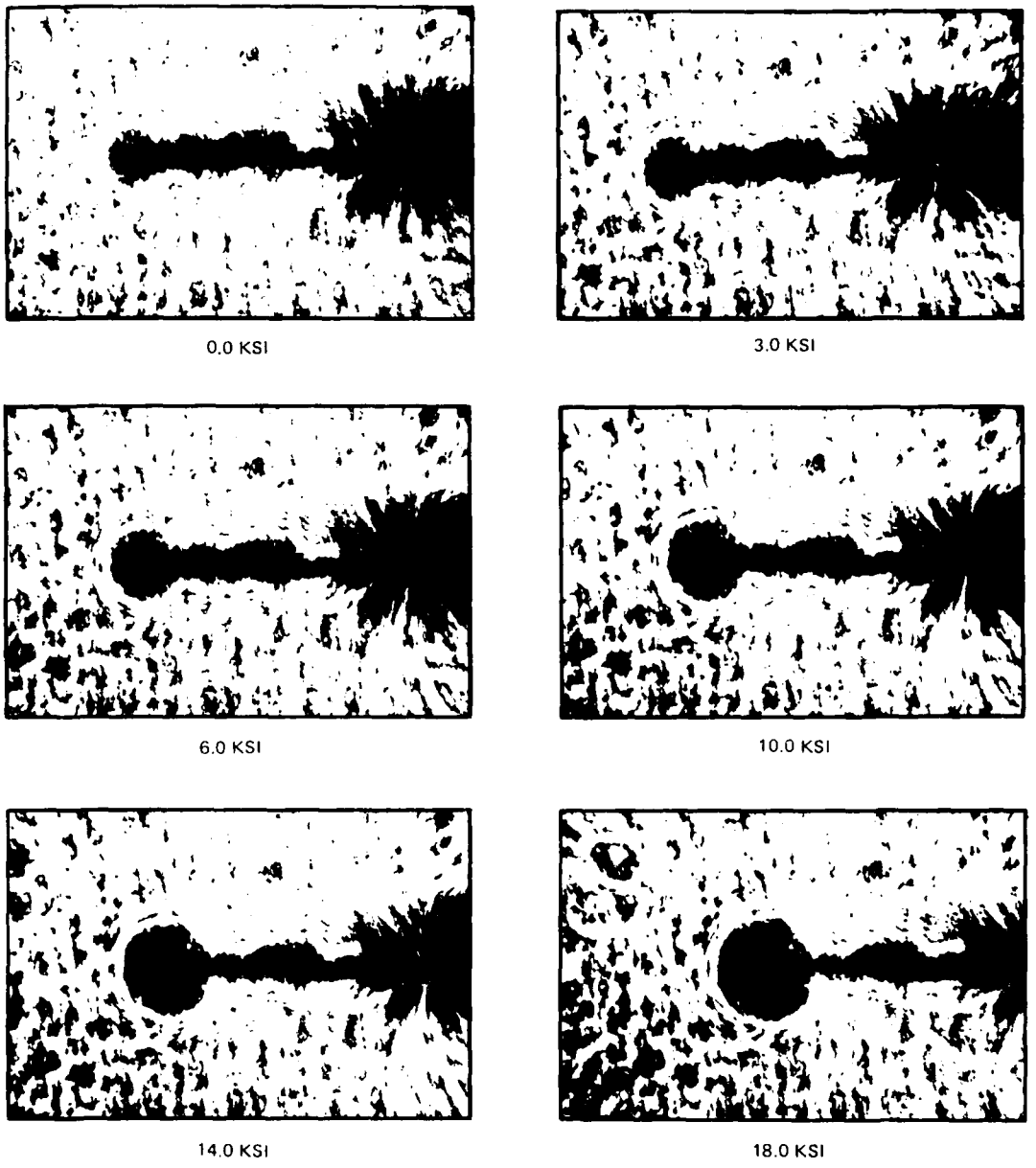

Fig. 2-8 Specimen 3C – Open Hole

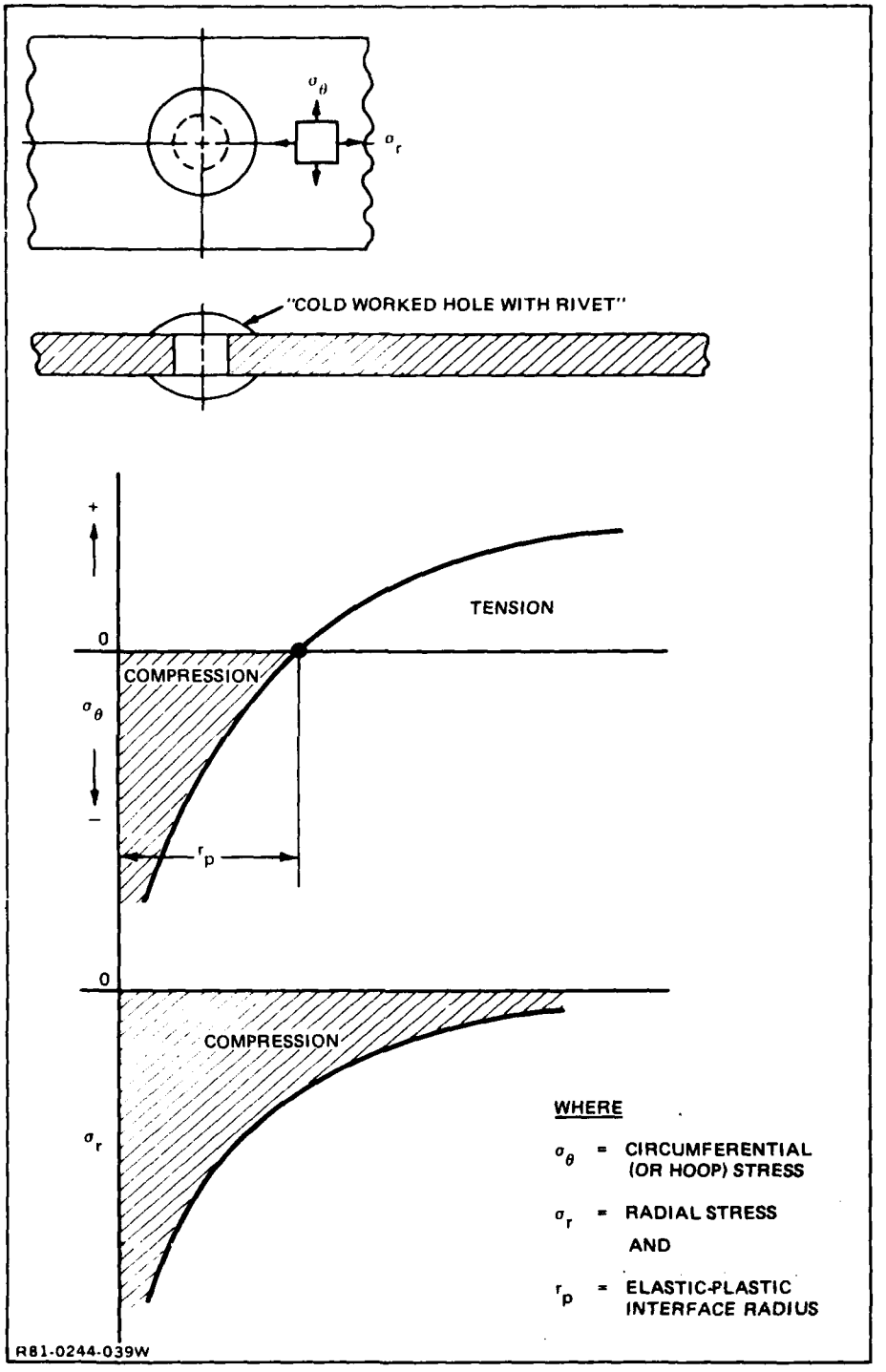

Fig. 2-9 Stresses in Cold Worked Hole with Rivet

hole exists prior to the cold working, with length $a < r_p$, a most desirable situation exists for high fatigue life enhancement, since the biaxial compression field will retard the crack growth. In this region, therefore, we expect to see a reduction in K_I values, in comparison with K_I values in precracked open holes, until the applied load on the specimen exceeds the residual stresses. If the crack length $a > r_p$, then the initial K_I values will be greater, after the cold working of the hole, than the K_I values obtained with the precracked open hole, but will remain constant until the applied loads in the specimen exceed the residual stresses.

A rivet was installed in the precracked hole which generated compressive residual stresses, not extensive enough so that $a > r_p$. Figure 2-10 represents the caustics of a precracked hole (described in the previous section) under load, before riveting (open hole). Figure 2-11 presents the caustic after cold working. Equation (40), which was derived earlier, to relate K_I with the major diameter of caustics applies to the results shown in Fig. 2-10, but it does not apply to the results shown in Fig. 2-11, because the conditions after riveting are no longer elastic. Plastic deformation has distorted the caustic in Fig. 2-11, but it did not eliminate it. In other cases, where the cold working is more extensive, and the cracks smaller (i.e., $a < r_p$) the caustic has completely vanished after riveting.

Finally, the rivet was drilled out. The residual tension hoop stress is now larger, causing an increase in the size of the caustic. Figure 2-12 presents the caustics at various loads for a precracked, cold worked hole under various loads. We can easily see that the sizes of the caustics in Fig. 2-12 under corresponding loads with the open hole results of Fig. 2-10, are larger and fatigue results can easily prove that in this case (i.e., where $a > r_p$) cold working has worsened the initial cracked hole conditions for fatigue life.

It is this qualitative comparison of experimental results in cold worked holes, that can be obtained by the method of caustics in a unique fashion. Cold working holes through riveting has been proven effective

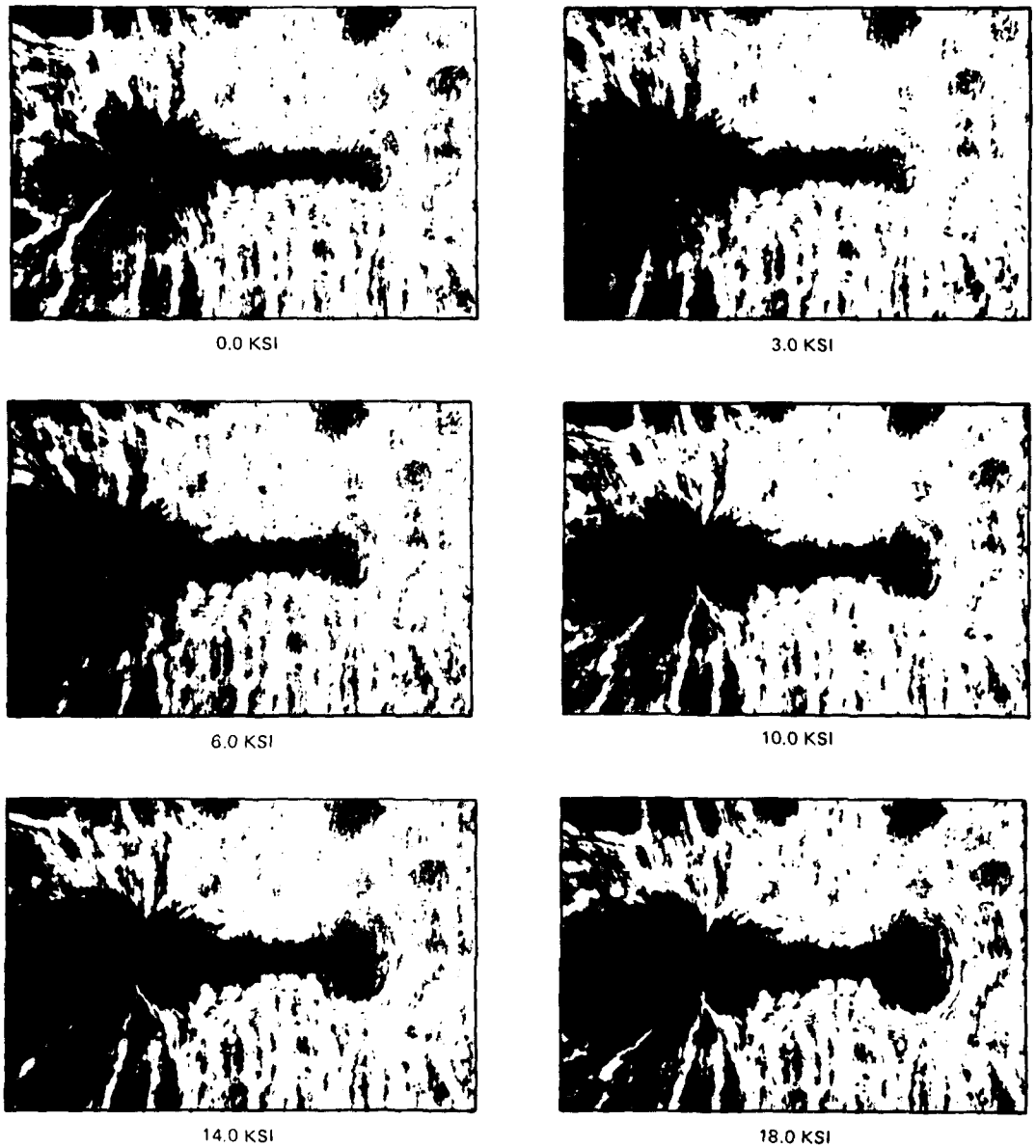

R81-0744-036W

Fig. 2-10 Specimen 3B – Open Hole

in fatigue life enhancement (i.e., increased by a factor of 20) of riveted joints, but care must be taken to provide the degree of cold work appropriate for the crack sizes we are trying to retard. The method of caustics gives us a means to evaluate difficult problems that usually are not easily amenable to analytical solutions. In addition, we can save valuable time in evaluating conditions before repairs, and provide a non-destructive means of evaluation after the repair of riveted joints.

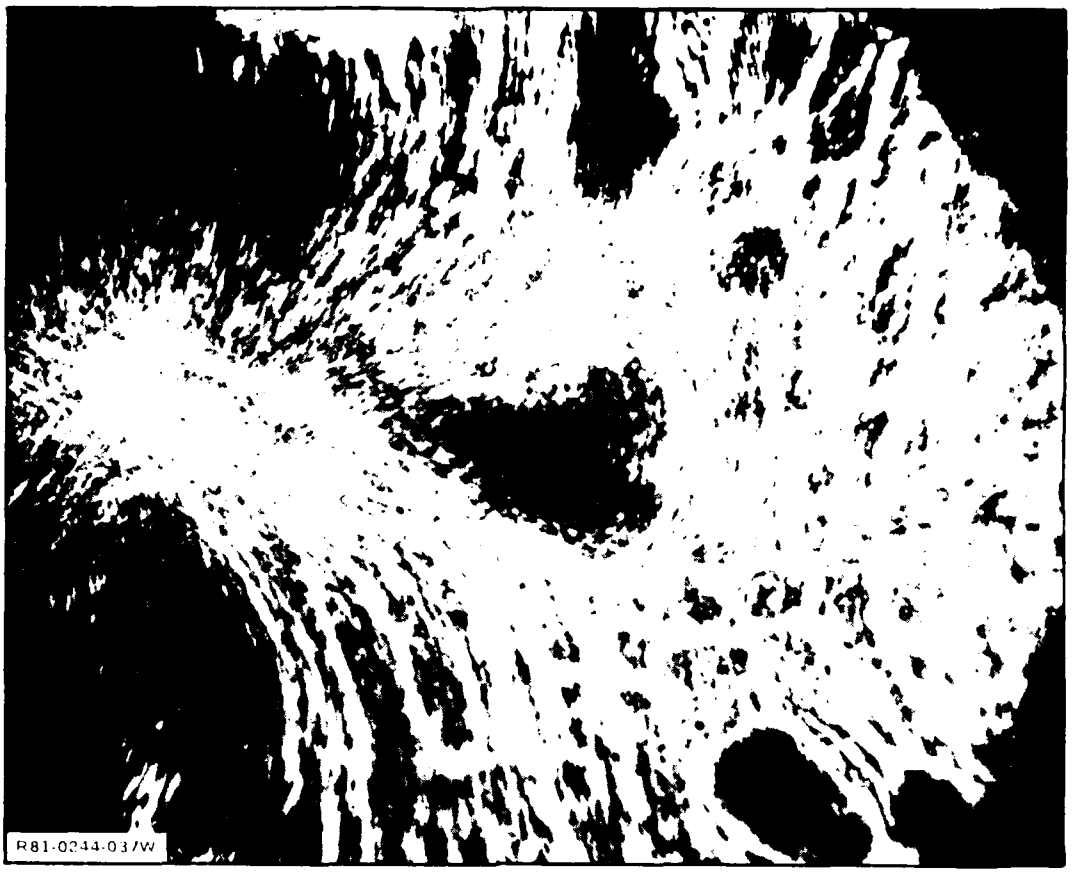

0.0 KSI

Fig. 2-11 Specimen 3B – Filled Hole – with Stress Wave Driven Rivet

0.0 KSI

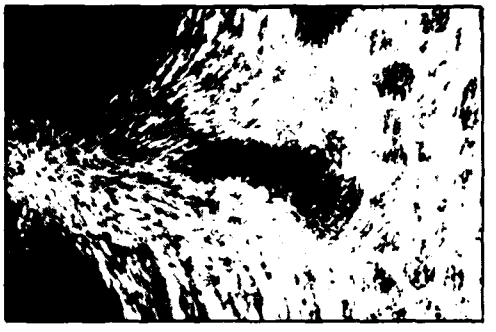

3.0 KSI

6.0 KSI

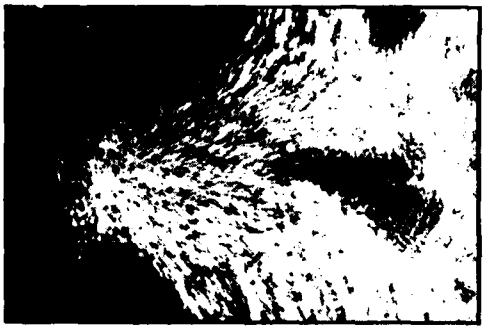

10.0 KSI

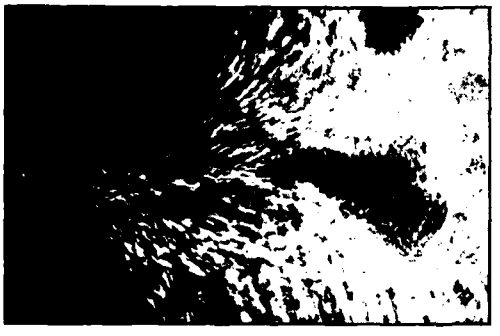

14.0 KSI

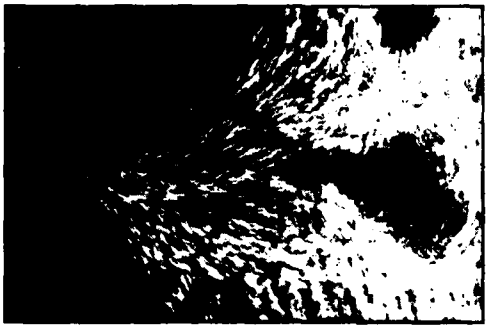

18.0 KSI

R81-0244-038W

Fig 2-12 Specimen 3B – Open Hole – After Removal of Stress Wave Driven Rivet

3. EXPERIMENTAL SET-UP

The experimental set-up used for this series of tests of the caustic phenomenon was assembled as a prototype system from equipment available in Grumman Aerospace Corporation's Experimental Mechanics Laboratory. This set-up is shown in Figs. 3-1 and 3-2.

The set-up consists of three basic components: a light conditioning assembly, a specimen loading frame, and a screen and camera to image and record the caustic display.

The light conditioning assembly is composed of a platform holding the optical components mounted on a combination of stages which allow controlled motion in the x-y-z directions, and rotation about the z axis. This flexibility is necessary to permit the axis of the light beam to be pointed at the crack on the test specimen. Image distortion takes place if the crack tip is located near the edges of the illuminated region of the specimen. The optical platform contains a 15 mW continuous wave helium/neon laser, beam steering mirrors, a spatial filter to expand the beam, a lens to collimate the expanding beam, and finally, a second lens to focus the beam on the specimen surface.

The loading frame is powered by an electric motor-driven screw jack. It features a rail-guided loading head, and a series of springs to permit increased accuracy in setting the desired load. Load magnitude is measured by a series of interchangeable calibrated load cells.

The magnitude of the stress intensity factor as determined by caustics is dependent on the diameter of the caustic on the image screen, and on the optical amplification factor chosen. To minimize possible errors due to these two factors, the following procedure was adopted. First, a black circle of known diameter was applied to the surface of each test specimen. When illuminated by the light beam, an amplified

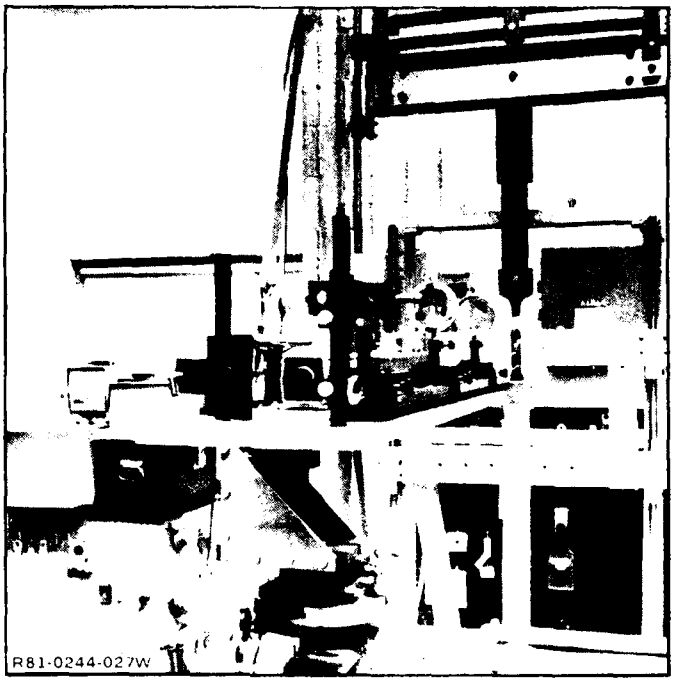

Fig. 3-1 Light Conditioning Assembly and Loading Frame

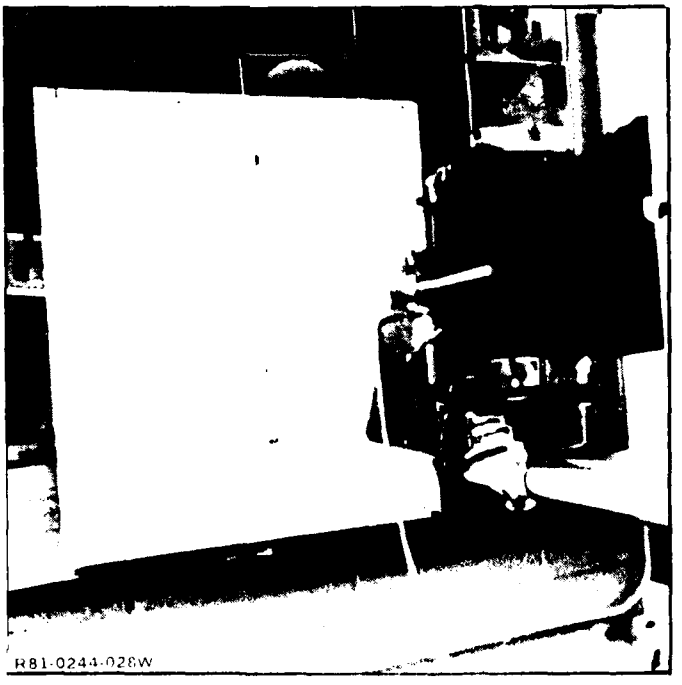

Fig. 3-2 Caustic Display and Camera

image of the circle is seen on the viewing screen. Since for these tests all measurements were to be made from photographs of the caustic images, the recording camera scale factor was obtained by photographing a quality steel scale. The combination of recording camera scale factor, and the ratio of the circle image size from its photograph to the actual circle size on the specimen, provides the optical amplification factor. Representative photographs of this procedure are shown in Fig. 3-3.

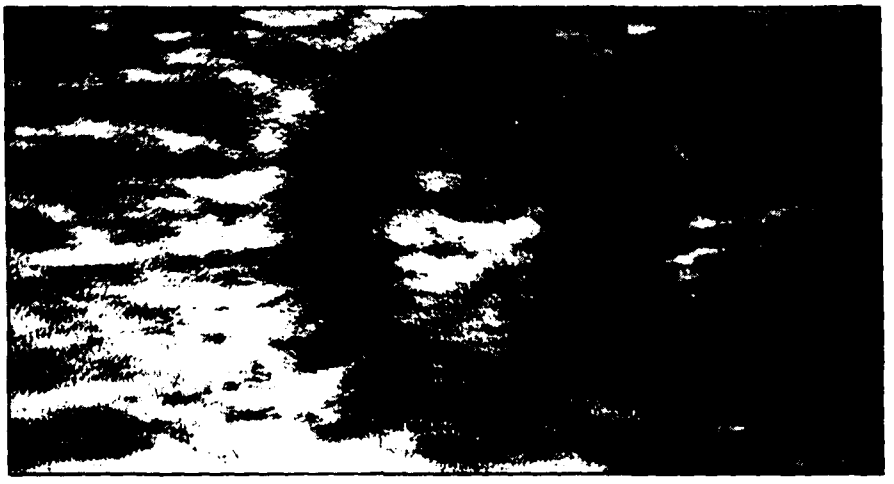

0.160 INCH DIAMETER TEST CIRCLE

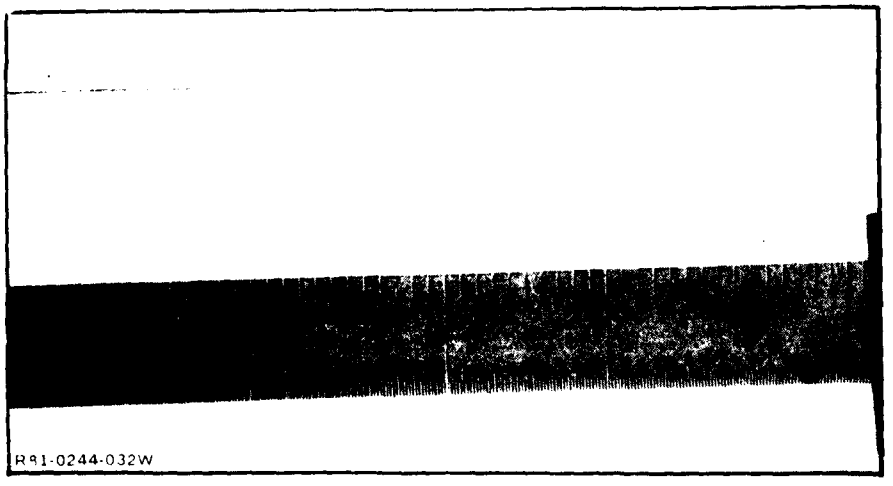

PHOTO SCALE FOR SPECIMEN 7

Fig. 3-3 Calibration and Photo Scale Shown Above Determine the Amplification Factor λ_m

4. DESCRIPTION OF EXPERIMENTS

This report contains the results of testing performed with seven 1-in. wide test specimens. The first four were 0.125-in. thick 2024-T851 aluminum alloy. The fifth specimen was 0.250-in. thick 2024-T851 aluminum alloy. The sixth was a 0.120-in. thick 4340V heat-treatable steel alloy normalized to 90 ksi tensile ultimate stress. Finally, number seven was also a 0.120-in. thick 4340V steel heat treated to 200 ksi tensile ultimate stress.

Specimen geometry is defined by Grumman Engineering Drawing number TGP-1075. A reduced size copy of this drawing is shown in Fig. 4-1. Hole faces were designated A, B and C on one side of each specimen, and D, E and F on the other, such that A/D, B/E and C/F were faces of the corresponding three holes.

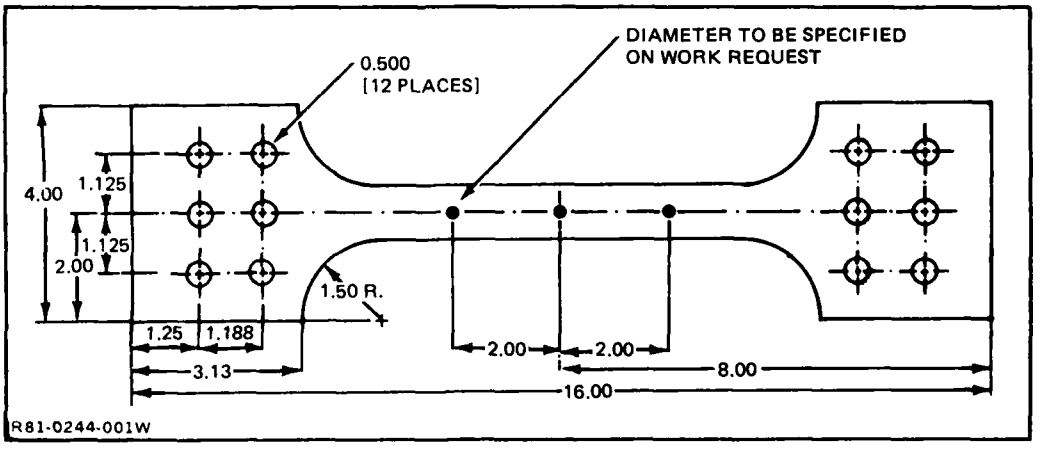

Fig. 4-1 Test Specimen

Specimens 2-7 were analyzed for both the cracked open-hole case, and for the cracked hole with an interference fit fastener installed.

DISCUSSION OF INDIVIDUAL EXPERIMENTS

Specimen No. 1

Material - 2024 T851

Width - 1.00 in.

Thickness - 0.125 in.

Hole Dia - 0.188 in.

Two test sequences were run with this test specimen. The first series of tests was conducted on the specimen in which the central hole had been cracked to 0.090 in. and then polished. The K_I values obtained by caustics were 50% lower than that predicted by the theoretical line. It was suspected that polishing after cracking was the cause of this error.

The cracks were extended for all three holes. The crack at the central hole grew from 0.090 in. to 0.200 in. into previously polished material. Correlation improved somewhat. Average value of K_I obtained by caustics was 77% of that predicted. Closer examination of these first caustics photographs indicated that the apparent caustic diameter is influenced by the position of the light beam relative to the crack tip. It was concluded that the light beam must be centered on the crack tip.

A re-run of the center hole was conducted with the light beam centered. The caustic diameters were read from the photographs three ways to obtain an estimate of possible scatter. The first reading employed the Laboratory's Fringe Reader, and electro-optical measuring system. The second reading was obtained by smoothing the edges of the caustic with a french curve. The final readings were obtained by smoothing the edges with an ellipse template. The results of these readings are presented in Fig. 4-2.

Finally, the upper and lower holes were loaded and photographed. These results are presented in Fig. 4-3.

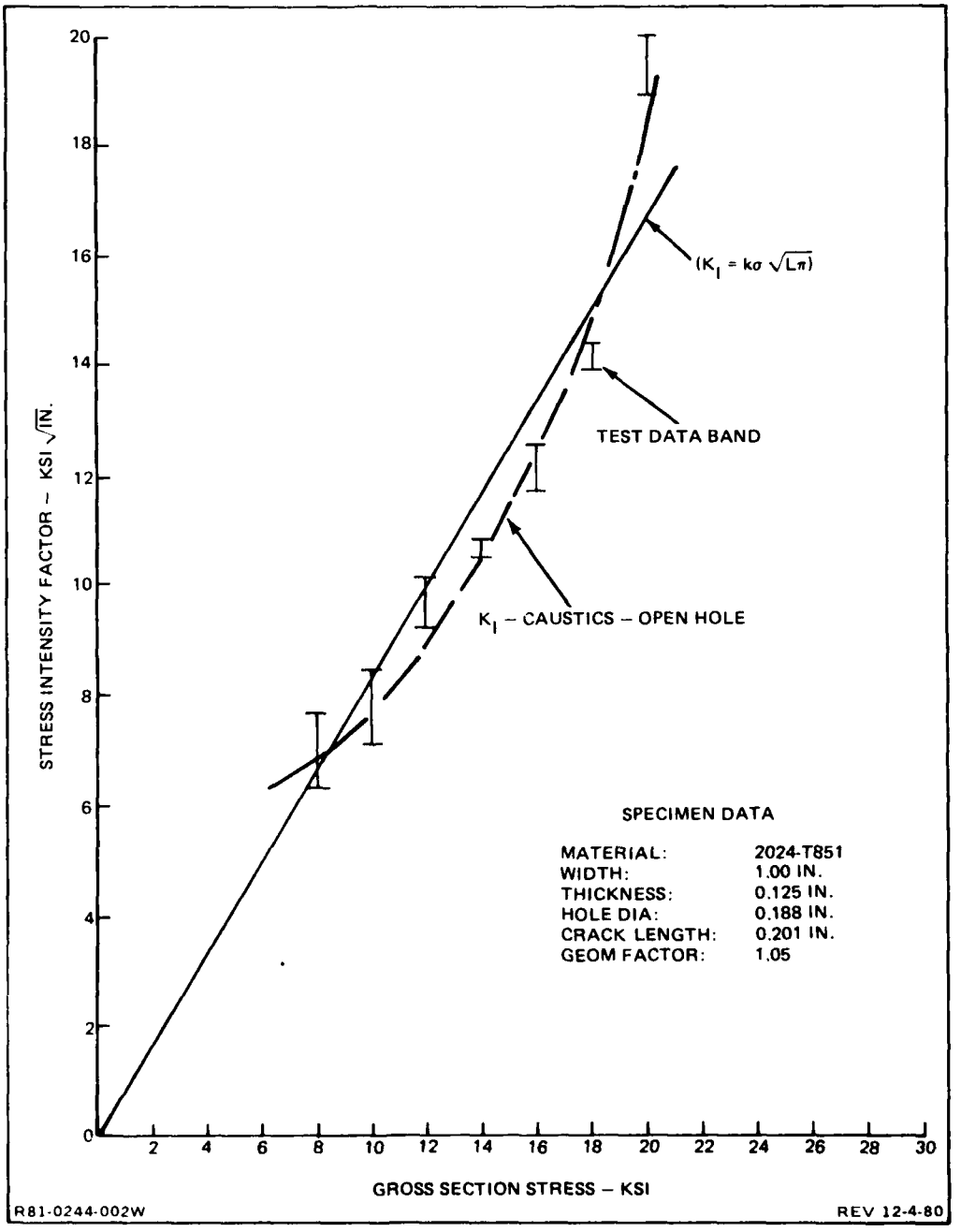

Fig. 4-2 Stress Intensity Factors (ksi $\sqrt{\text{in.}}$), Caustics vs Theory, Specimen No. 1, Center Hole

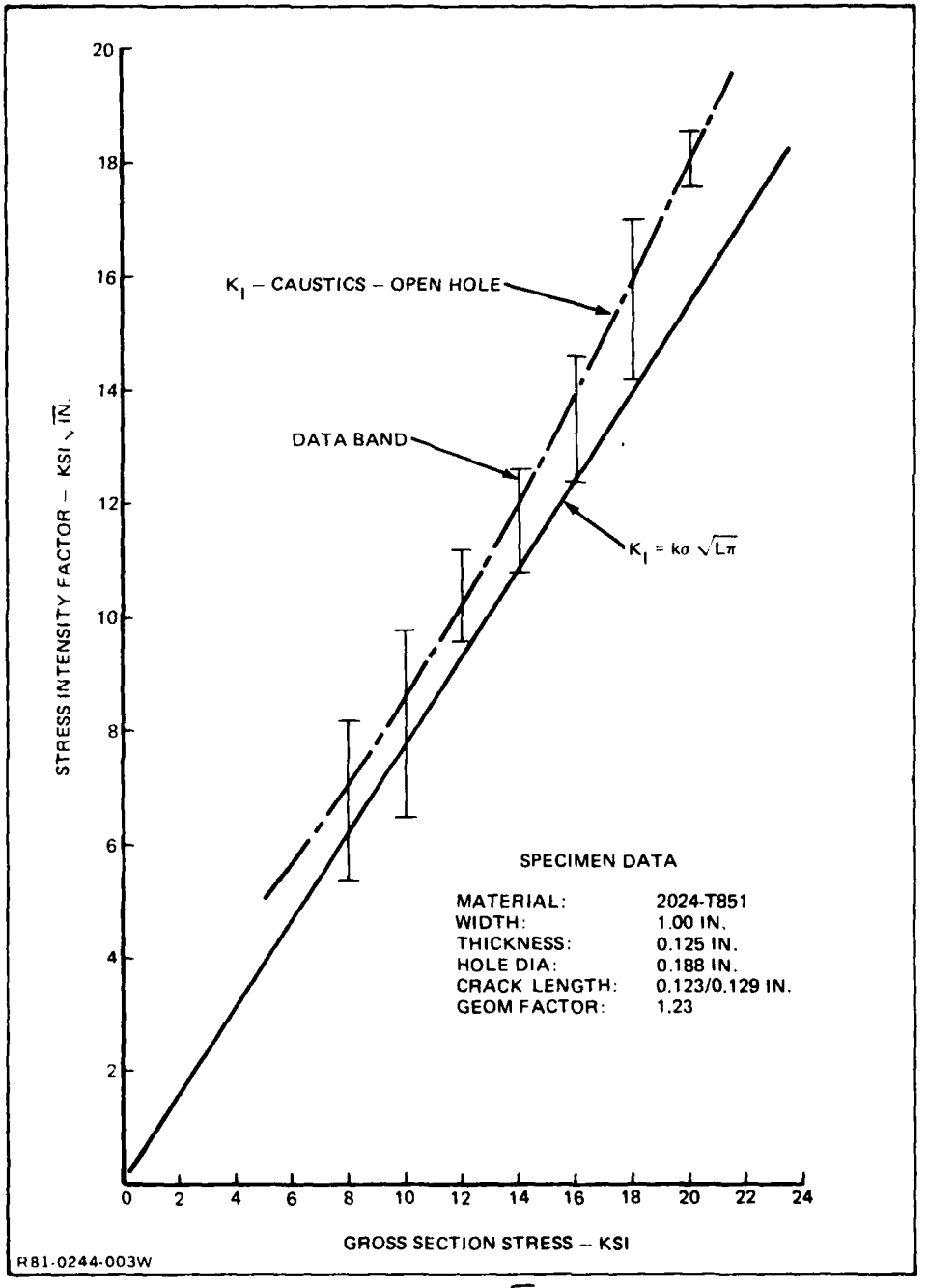

Fig. 4-3 Stress Intensity Factors (ksi $\sqrt{\text{in.}}$), Caustics vs Theory, Specimen No. 1, Upper and Lower Holes

Specimen No. 2

Material - 2024-T851

Width - 1.000 in.

Thickness - 0.125 in.

Hole Dia - 0.191 in.

Open hole data were obtained for hole faces, A, B, E and F. These four crack faces had crack lengths of 0.013 to 0.045 in., which have geometry factors ranging from 2.58 to 1.78. The K_I values obtained by caustics were all significantly lower than predicted. These open hole results are presented in Figs. 4-4 through 4-7.

Steel rivets were driven into the three holes using 0.063-in. thick aluminum cover plates. Examination of the crack zones indicated that despite the use of cover plates, the riveting process had crushed the surface enough to mask the crack and the crack tip caustics.

The cracks were extended approximately 0.025 - 0.050 in. Once again the specimen was examined in the caustics set-up, but the caustics were still not visible.

The cracks were extended one more time by approximately 0.025 - 0.050 in. The final crack lengths ranged from 0.008 - 0.162 in. The caustics produced, where visible, were of a quality which precluded their use.

Specimen No. 3

Material - 2024-T851

Width - 1.00 in.

Thickness - 0.125 in.

Hole Dia - 0.125 in.

Open hole data were obtained for hole faces B, C, E and F, which had crack lengths of 0.134 - 0.168 in. The geometry factors ranged from

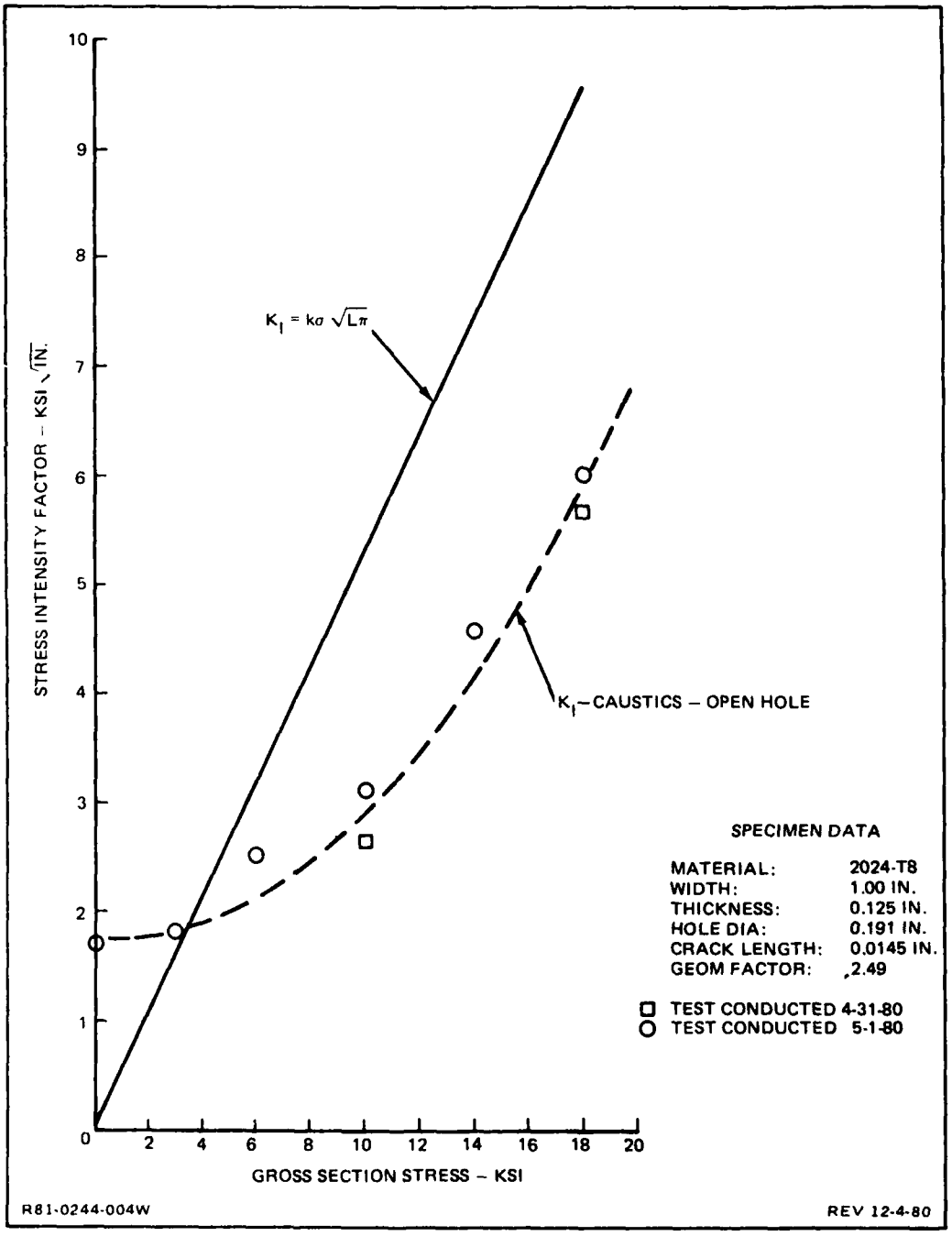

Fig. 4-4 Stress Intensity Factors (ksi $\sqrt{\text{in.}}$), Caustics vs Theory, Specimen 2A

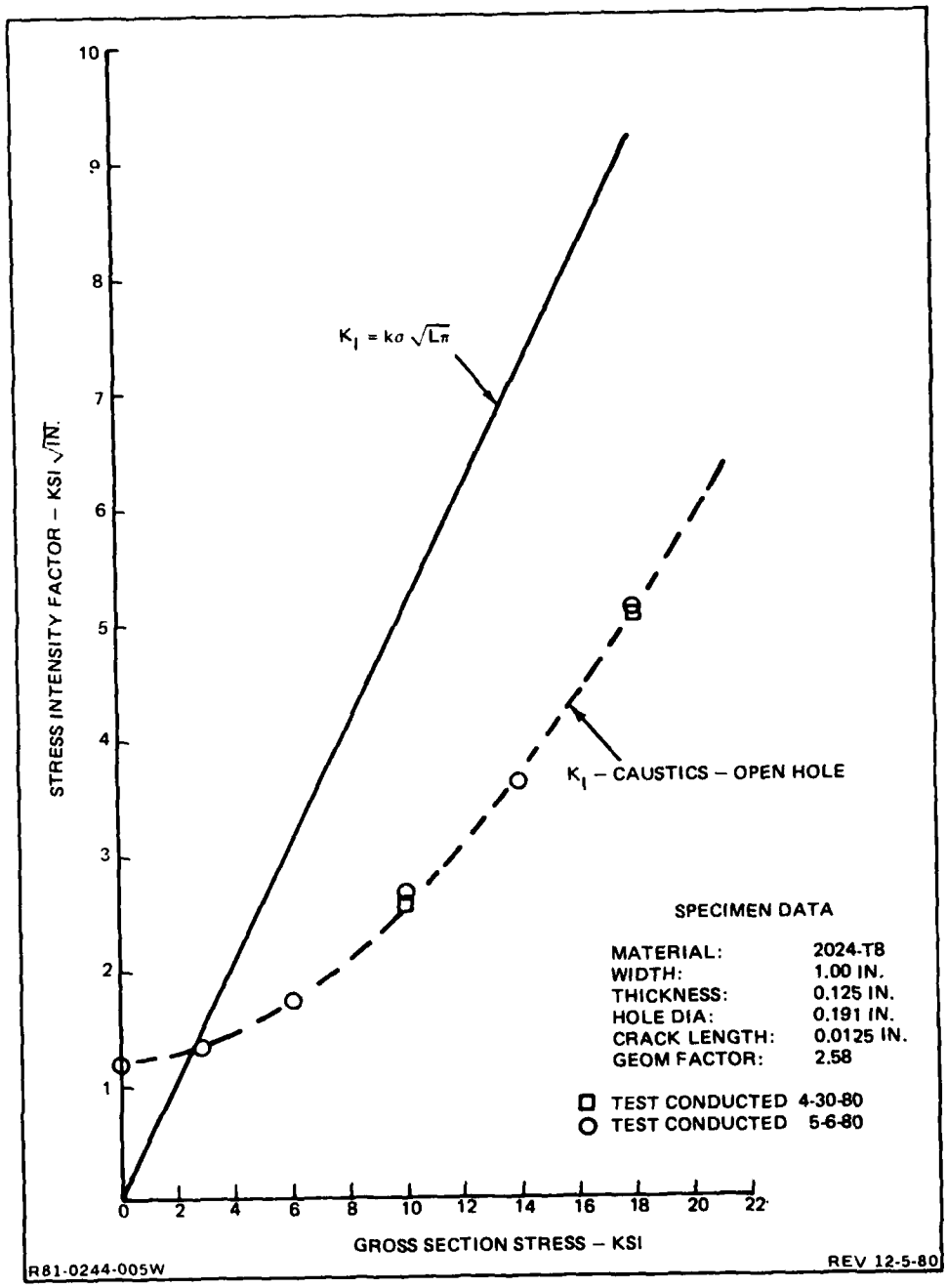

Fig. 4-5 Stress Intensity Factors (ksi $\sqrt{\text{In.}}$), Caustics vs Theory, Specimen 2B

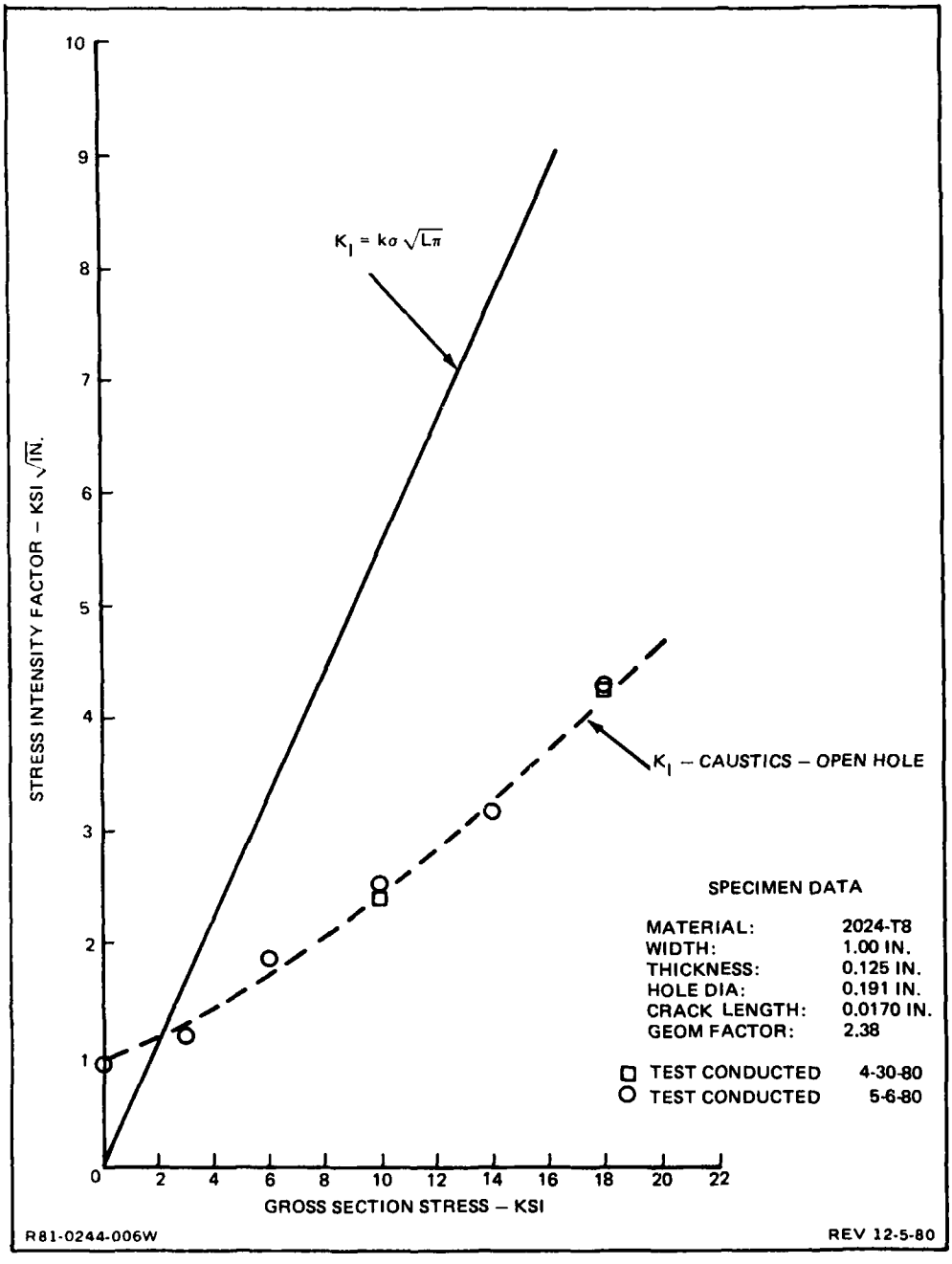

Fig. 4-6 Stress Intensity Factors (ksi $\sqrt{\text{in.}}$), Caustics vs Theory, Specimen 2E

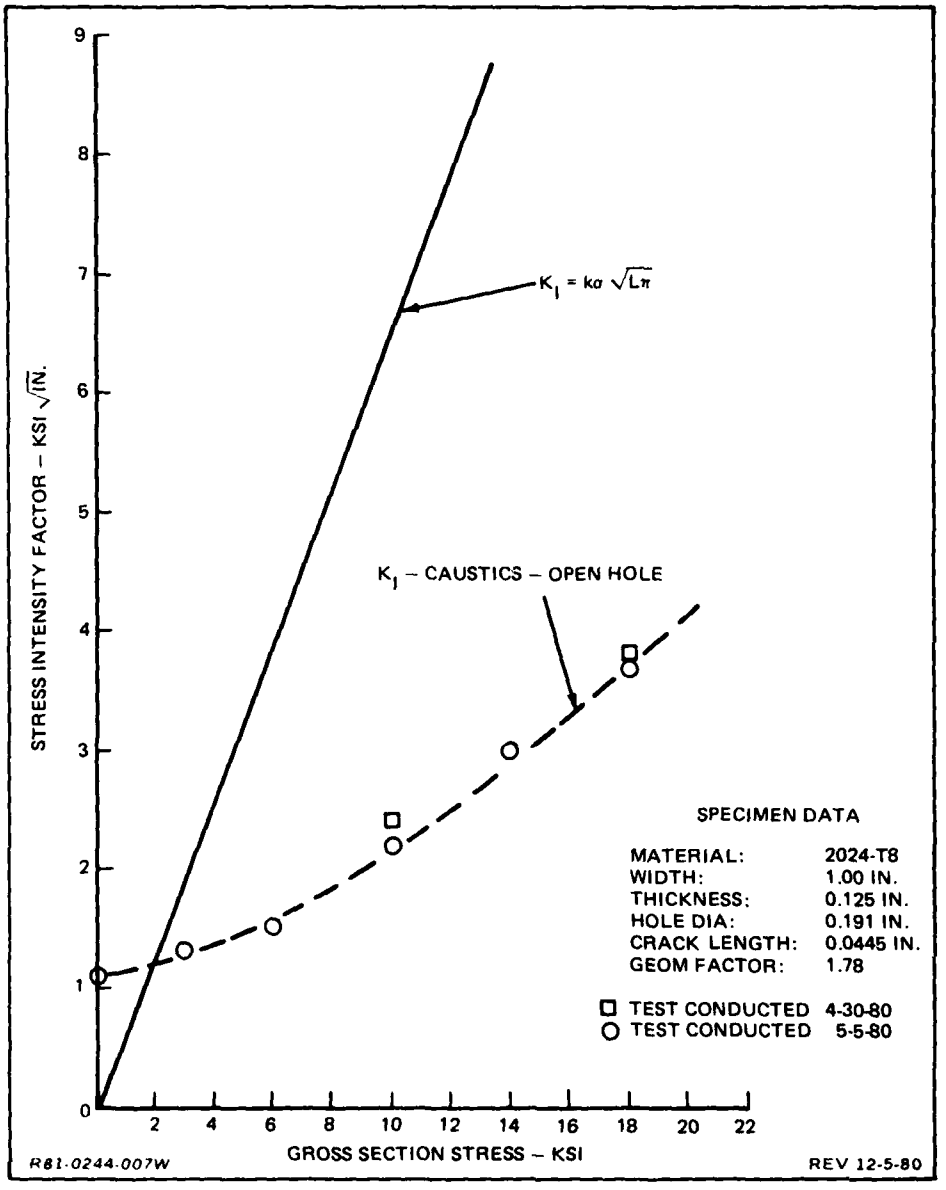

Fig. 4-7 Stress Intensity Factors (ksi $\sqrt{\text{in.}}$), Caustics vs Theory, Specimen 2F

1.00 to 0.98. As shown in Figs. 4-8, 4-9, and 4-10, reasonable correlation between the predicted values of K_I and the values obtained by the caustics method were obtained for hole faces B, C and E. Hole face F was very different, and produced a K_I curve much like those produced by Specimen 2, as shown in Fig. 4-11.

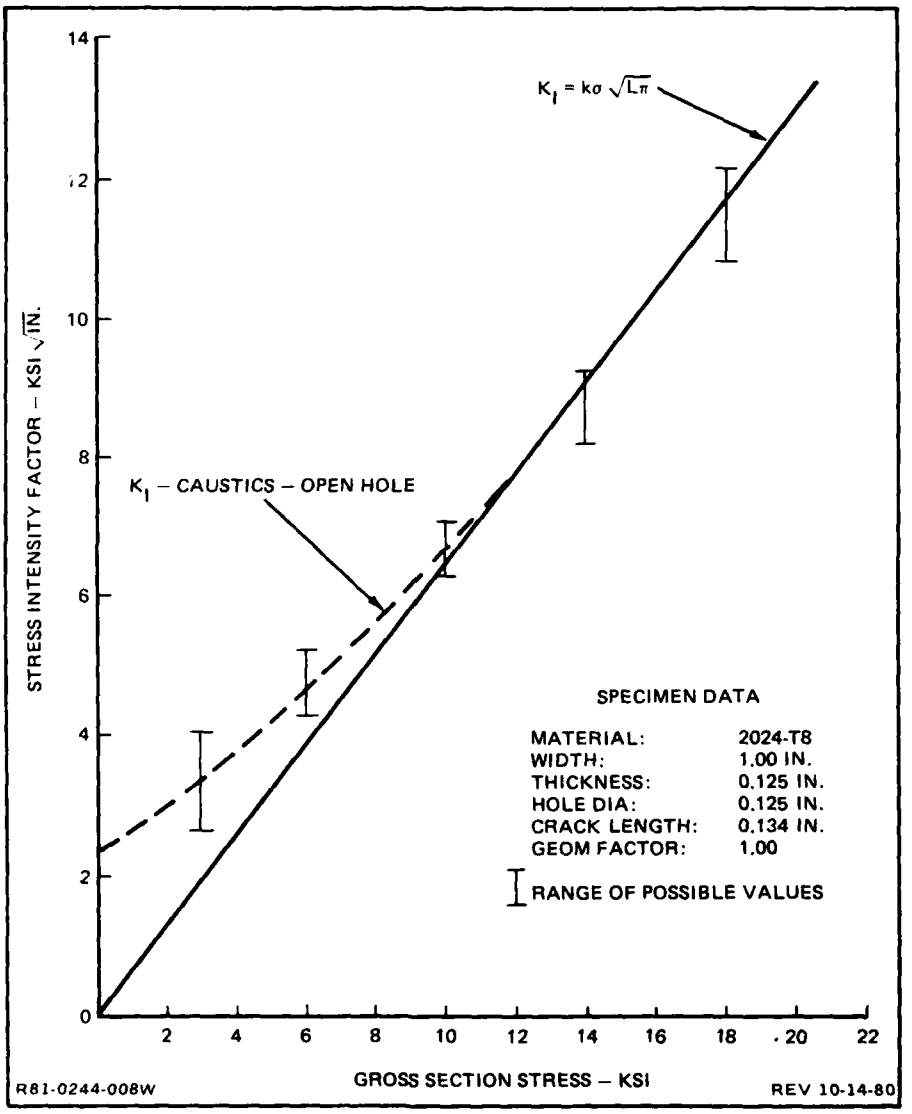

Fig. 4-8 Stress Intensity Factors (ksi $\sqrt{\text{in.}}$), Caustics vs Theory, Specimen 3B

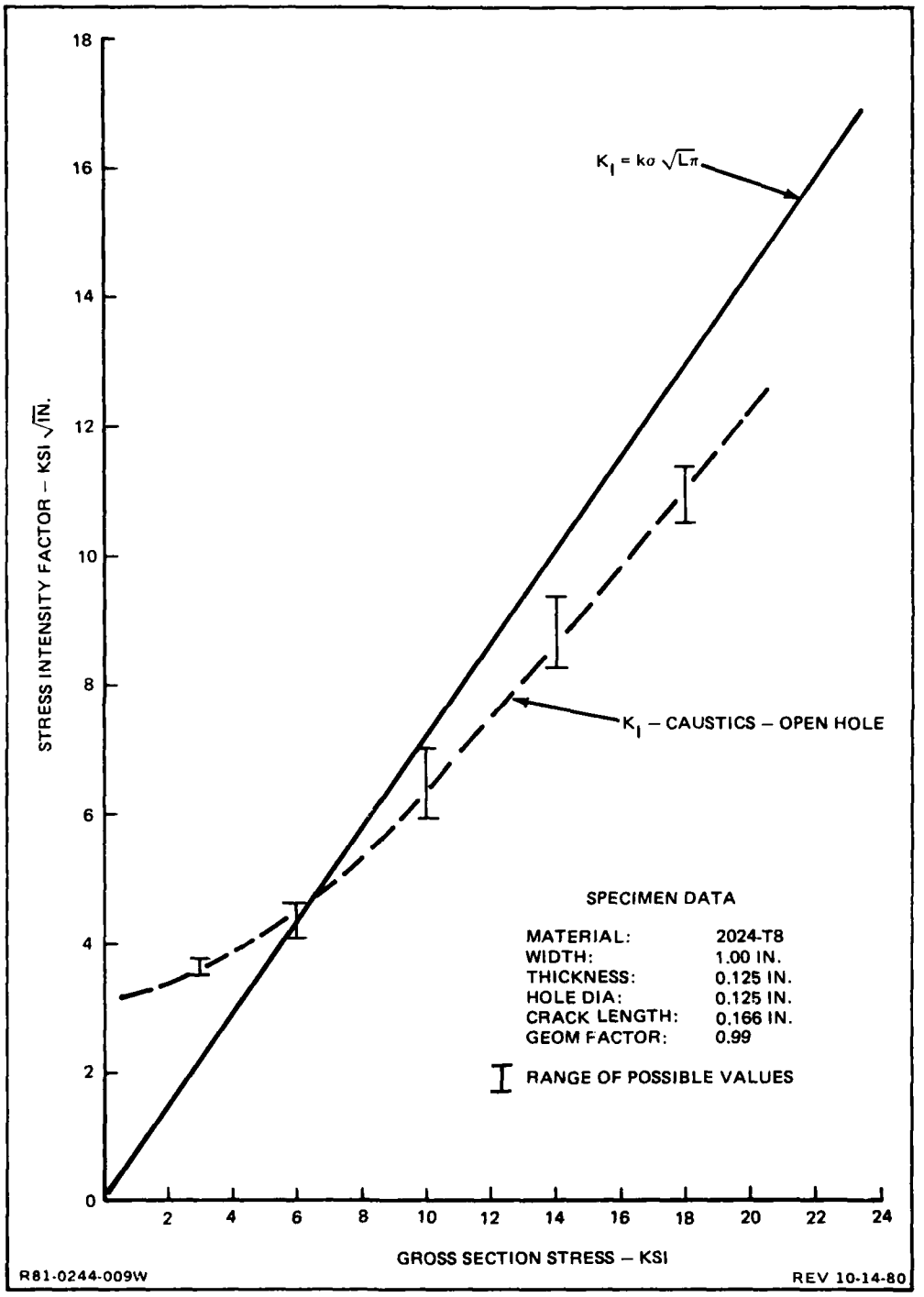

Fig. 4-9 Stress Intensity Factors (ksi $\sqrt{\text{in.}}$), Caustics vs Theory, Specimen 3C

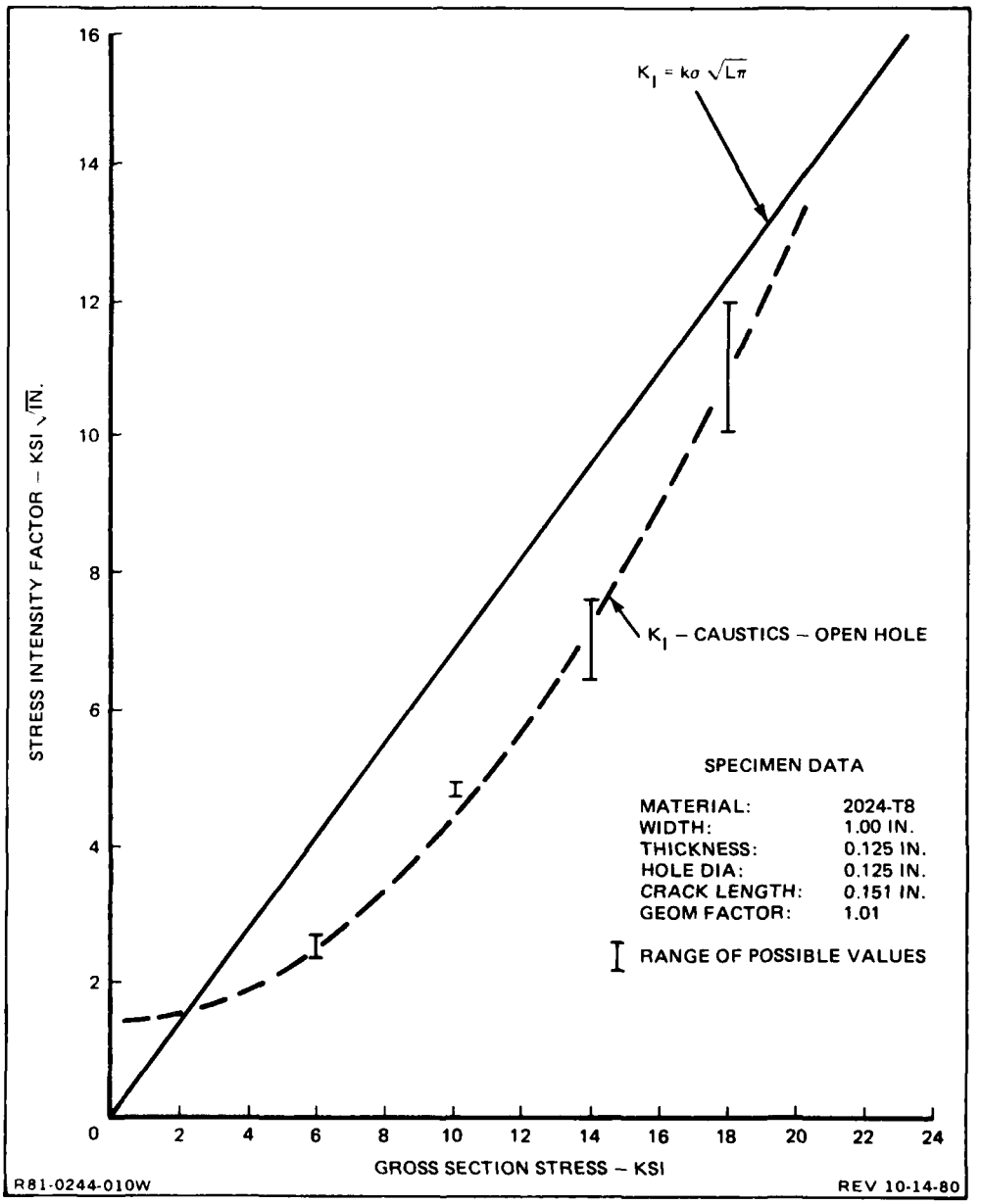

Fig. 4-10 Stress Intensity Factors (ksi $\sqrt{in.}$), Caustics vs Theory, Specimen 3E

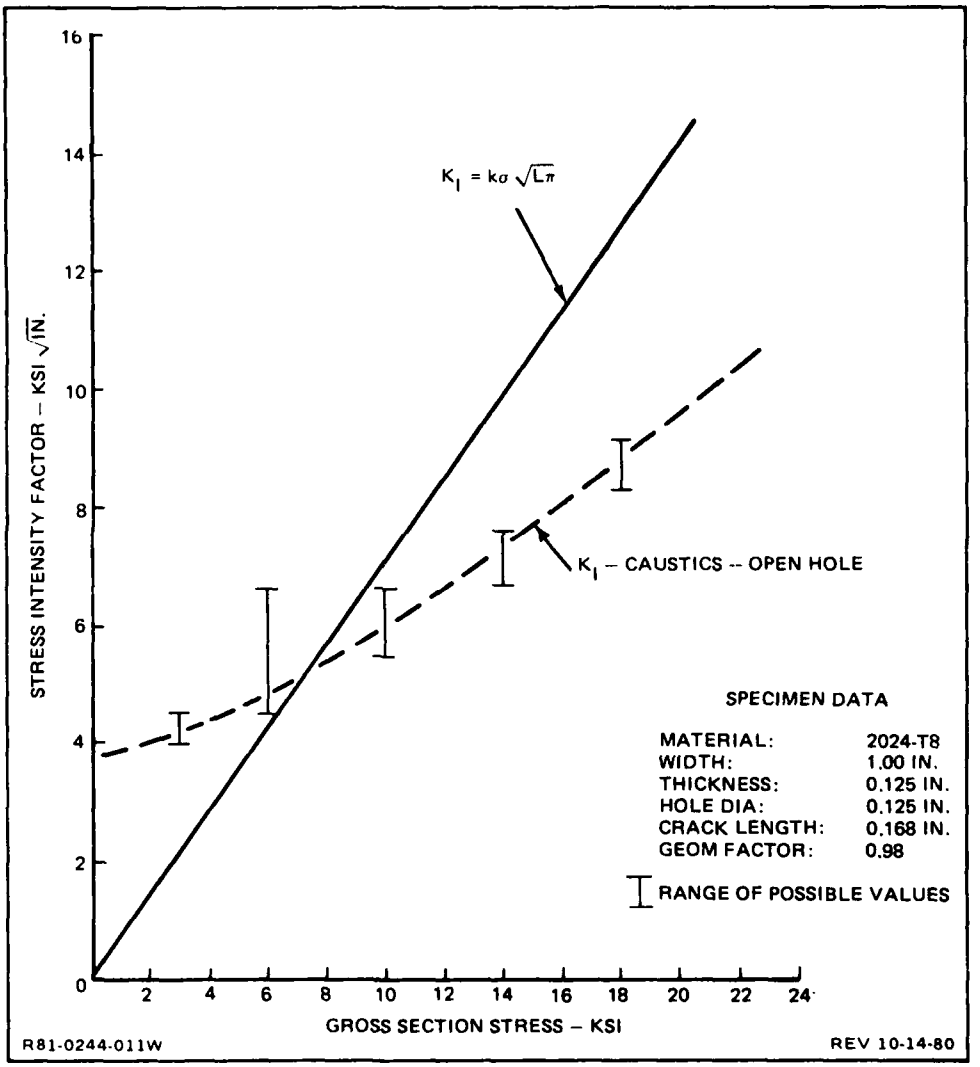

Fig. 4-11 Stress Intensity Factors (ksi $\sqrt{\text{in.}}$), Caustics vs Theory, Specimen 3F`

Hole faces B/E and C/F were enlarged to 0.191 in. diameter, and steel rivets with an initial 0.001 in. diametral interference installed. The rivet in hole B/E was upset using the 6-in. Stress Wave Riveter at 5.5 kilovolts (kv). The rivet in hole C/F was upset at 7.0 kv. The faces of the specimen were protected locally with 1/8-in. thick rubber pads during the riveting operation. With the rivets in place large static residual caustics were observed at faces B and F. The equivalent K_I were:

For hole face B, K_I = 16,133 psi $\sqrt{in.}$

For hole face F, K_I = 85,054 psi $\sqrt{in.}$

There was evidence of residual caustics at hole faces C and E, but the patterns were not sufficiently clear to allow the K_I values to be determined.

The rivets were removed, and it was noted that the static residual caustics reduced in size to:

For hole face B, K_I = 14,399 psi $\sqrt{in.}$

For hole face F, K_I = 28,497 psi $\sqrt{in.}$

Finally, hole face B was loaded incrementally to a gross section stress of 18 ksi, and the K_I values plotted. Figure 4-12 shows the K_I value remained constant at 14,399 psi $\sqrt{in.}$ between 0 and 10 ksi, then increased linearly to 23,157 psi $\sqrt{in.}$ at 18 ksi.

Specimen No. 4

Material - 2024-T851

Width - 1.000 in.

Thickness - 0.125 in.

Hole Dia - 0.190 in.

Open-hole data were obtained for all six faces on this specimen. The crack lengths varied from 0.039 - 0.060 in., with geometry factors of 1.85 - 1.58. Above 4 ksi, the K_I obtained by caustics was less

than, or in one case (4D) approximately equal to, the values predicted theoretically. These results are plotted in Figs. 4-13 through 4-18.

Steel rivets were installed in holes B/E and C/F. The rivet in hole B/E was driven with the 6-in. Stress Wave Riveter (SWR) hit on both sides at 5.5 kv. The residual stress field surrounding the rivet was high enough to completely mask the caustic patterns. The rivet in hole C/F was driven with the 6-in. SWR hit on one side only at 5.5 kv. It was observed that the F face of the specimen became concave (i.e., the overall field reflection became smaller), and neither the crack nor

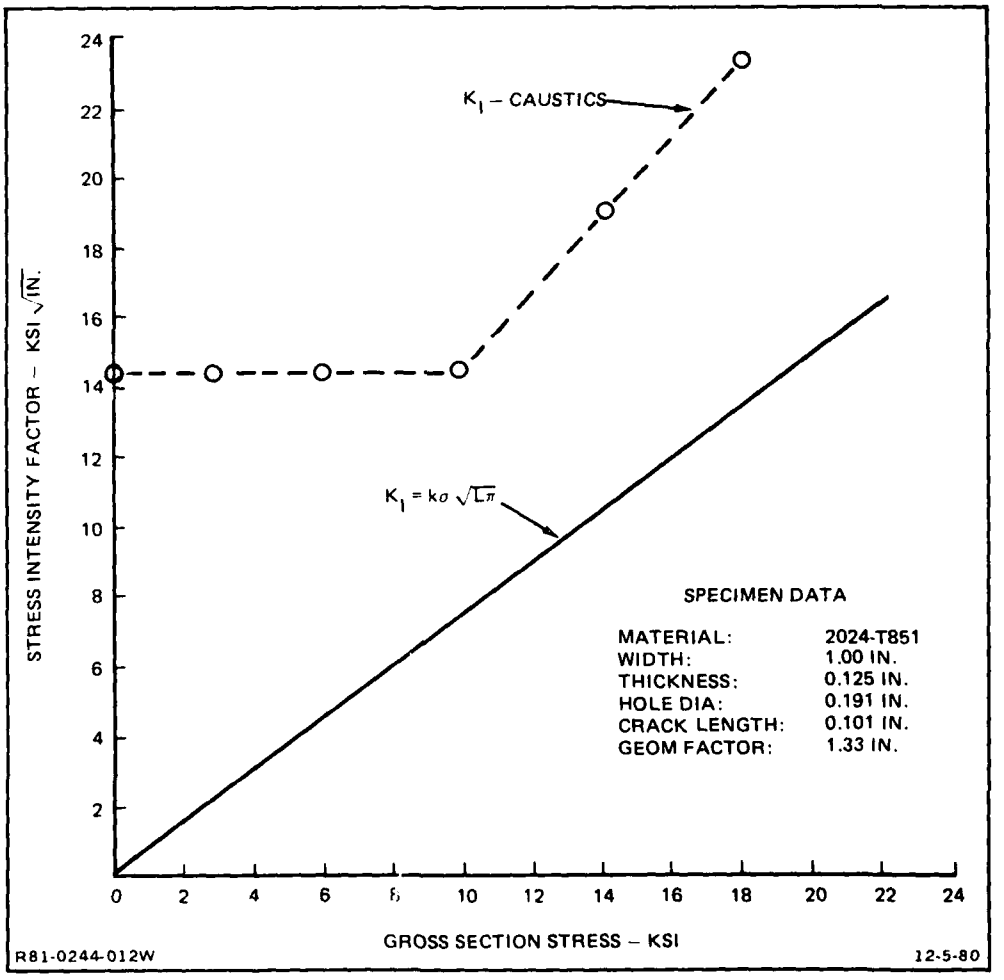

Fig. 4-12 Stress Intensity Factors (ksi $\sqrt{\text{in.}}$) Caustics vs Theory, Specimen 3B After Removal of Rivet

the crack tip caustic were visible. The C face became convex. A zero-load crack tip caustic approximately equal to the open hole caustic at 18 ksi was visible. This caustic did not vary in size for gross section stresses from 0-18 ksi.

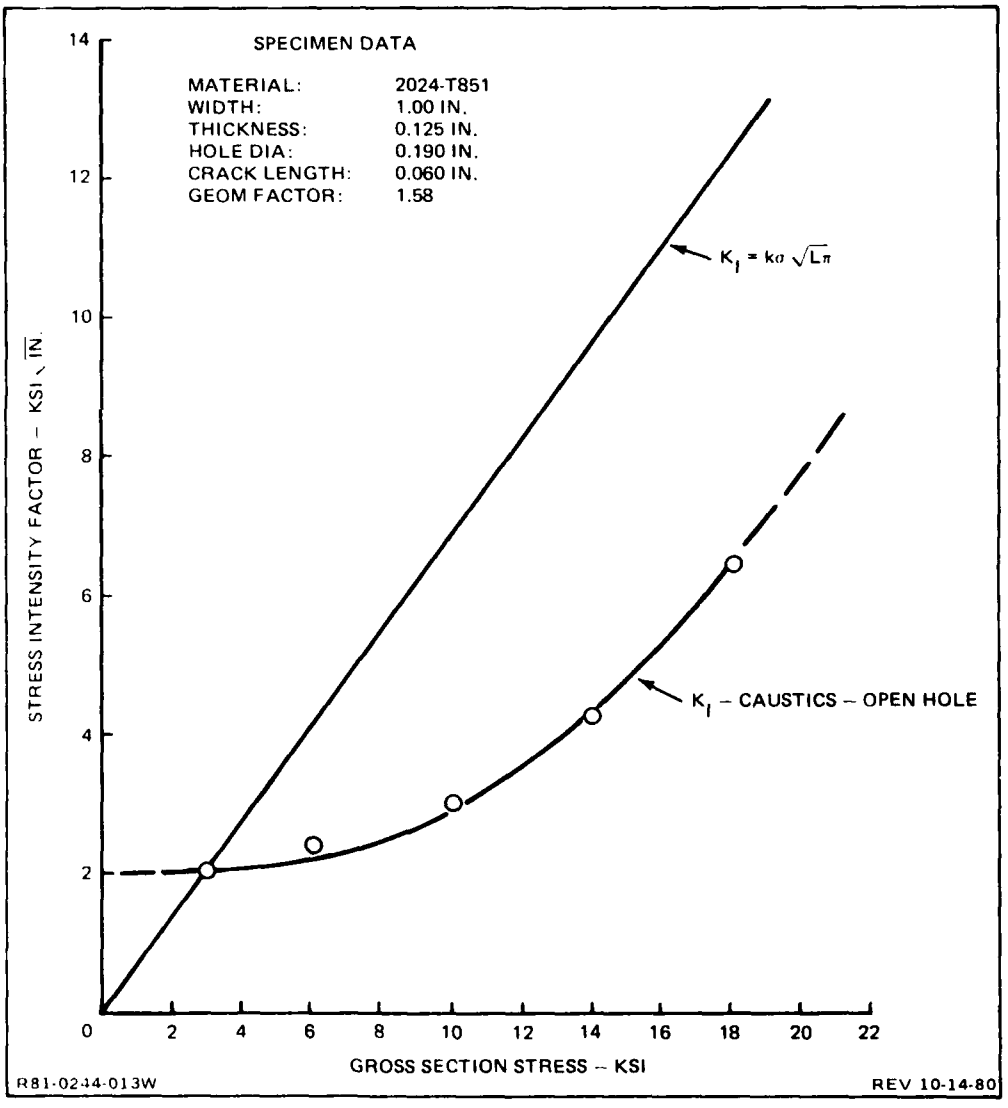

Fig. 4-13 Stress Intensity Factors (ksi $\sqrt{\text{in.}}$), Caustics vs Theory, Specimen 4A

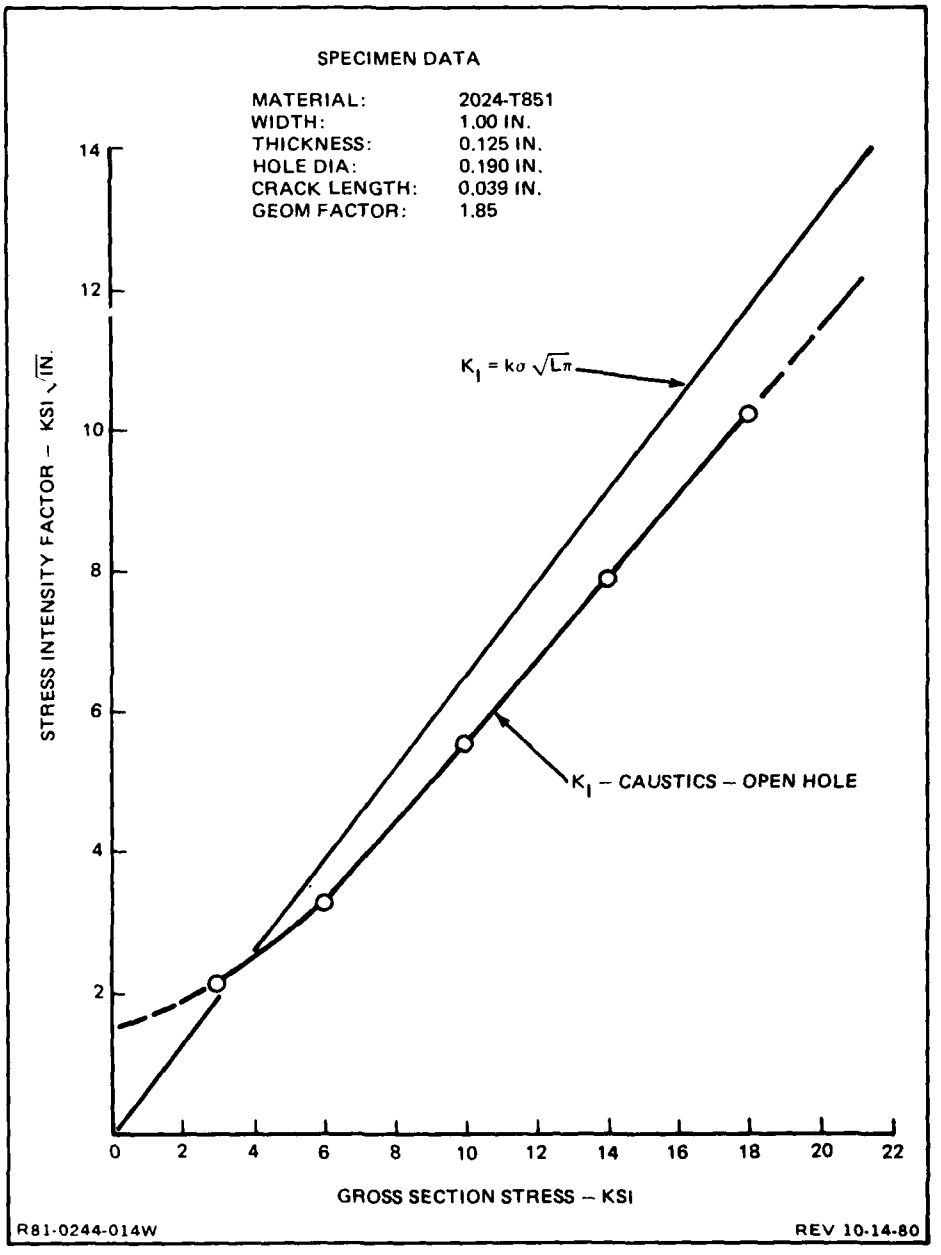

Fig. 4-14 Stress Intensity Factors (ksi $\sqrt{\text{in.}}$), Caustics vs Theory, Specimen 4B

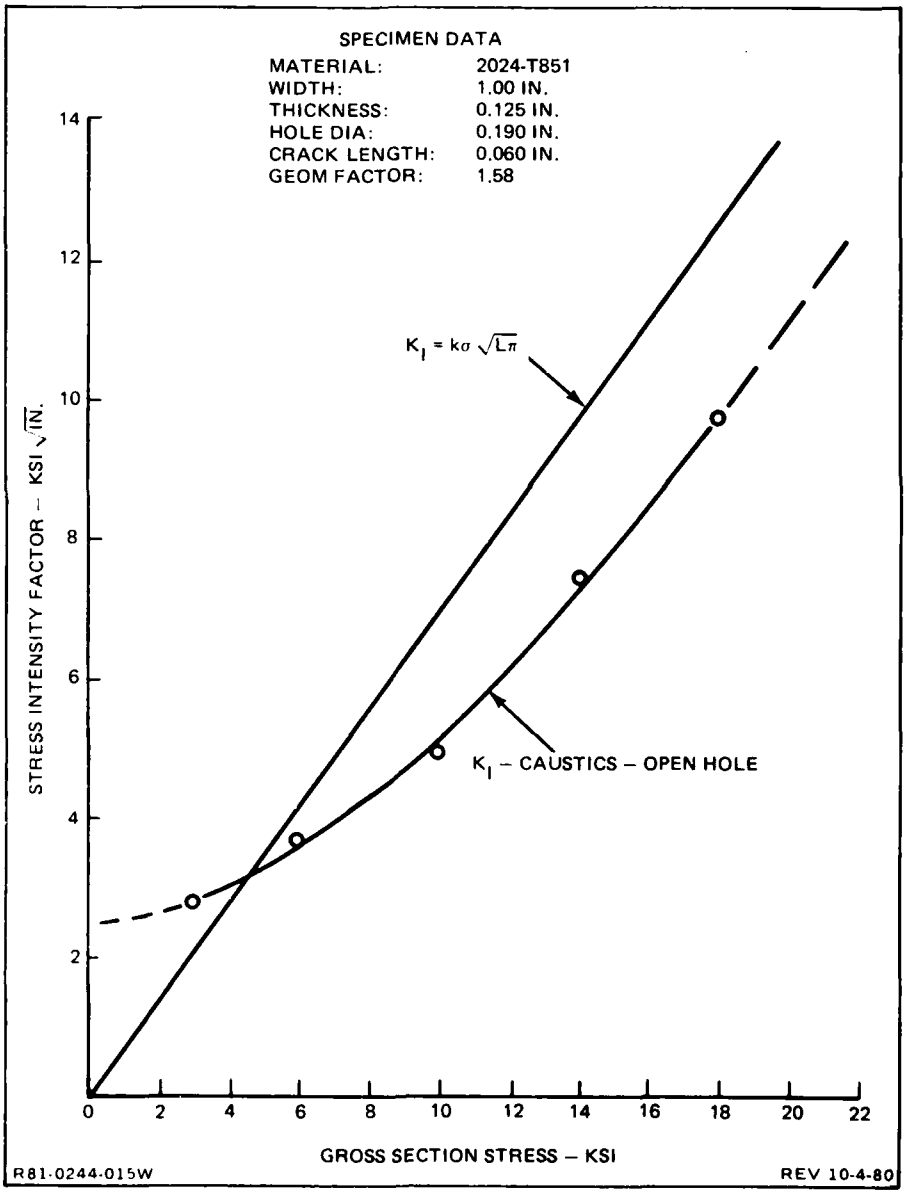

Fig. 4-15 Stress Intensity Factors (ksi $\sqrt{\text{In.}}$), Caustics vs Theory, Specimen 4C

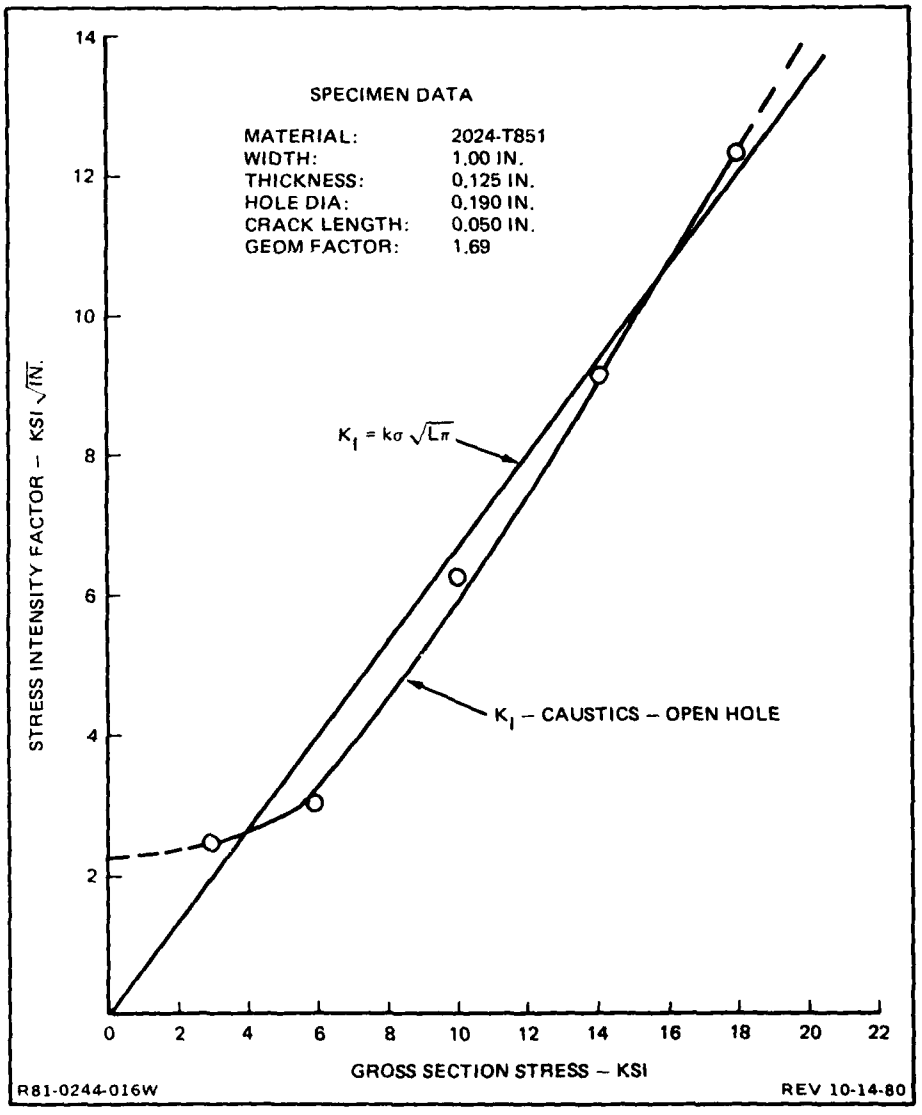

Fig. 4-16 Stress Intensity Factors (ksi $\sqrt{\text{in.}}$), Caustics vs Theory, Specimen 4D

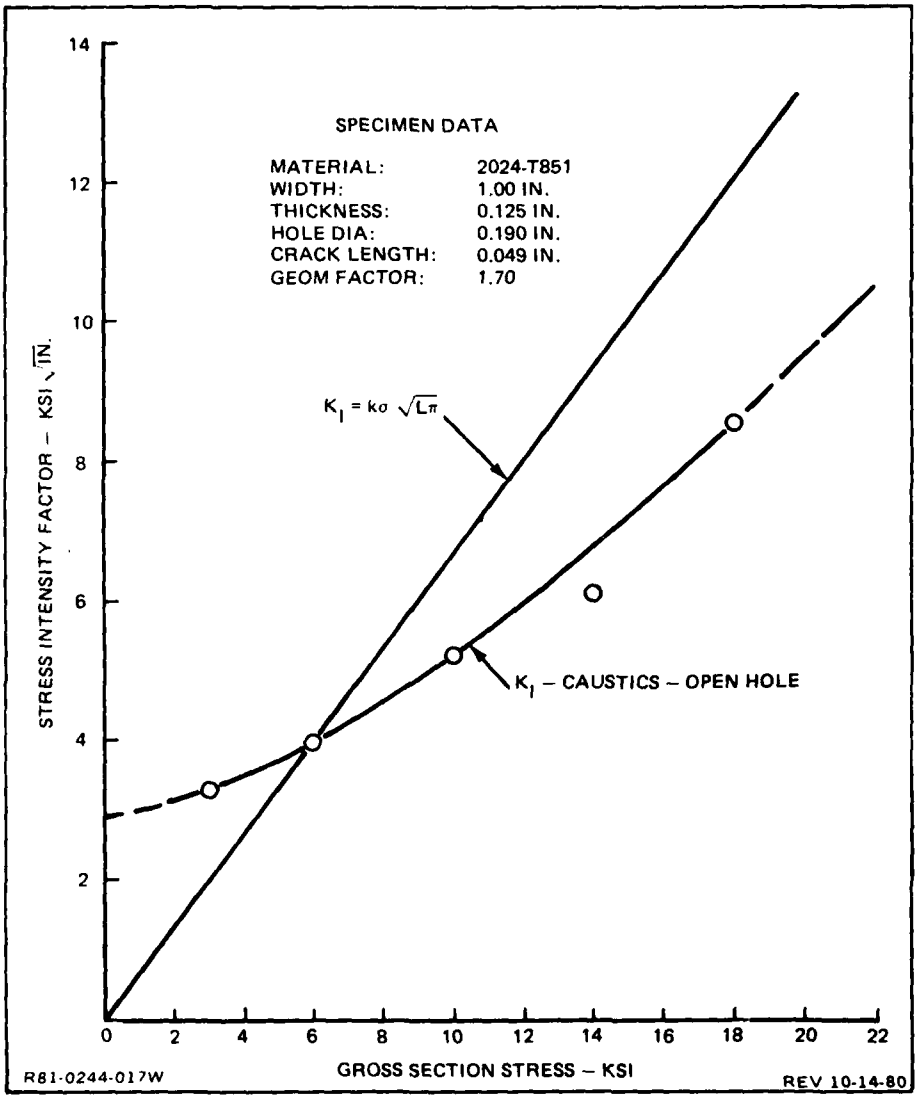

Fig. 4-17 Stress Intensity Factors (ksi $\sqrt{in.}$), Caustics vs Theory, Specimen 4E

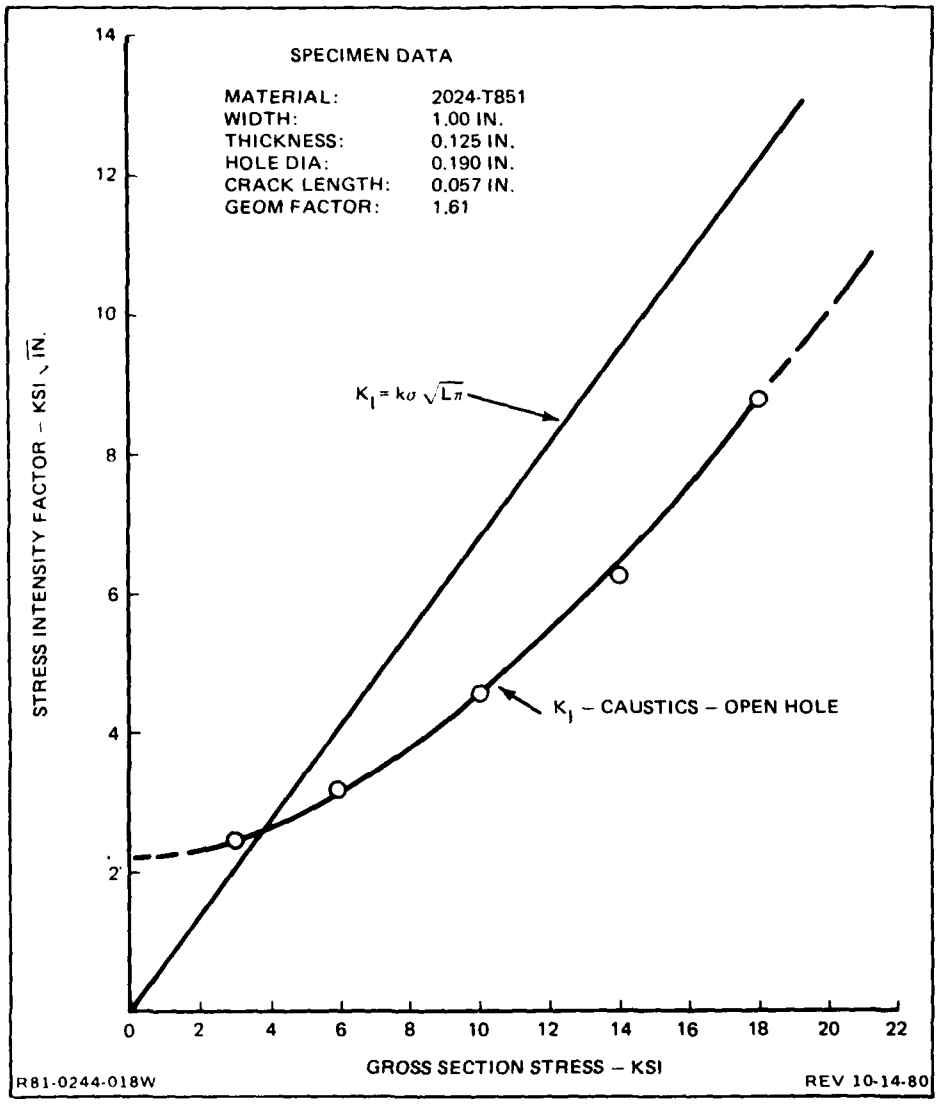

Fig. 4-18 Stress Intensity Factors (ksi $\sqrt{\text{in.}}$), Caustics vs Theory, Specimen 4F

Specimen No. 5

Material - 2024-T851

Width - 1.000 in.

Thickness - 0.250 in.

Hole Dia - 0.191 in.

Cracks lengths of 0.045 - 0.048 in. were obtained on one side of the specimen only (i.e., these were corner cracks). Open hole caustics were recorded for hole faces A and B. Face C did not produce a caustic due to a scratch mark on the specimen made during handling. For a corner crack, the theoretical line is defined by:

$$K_I = k\sigma \sqrt{L\pi}$$

where:

$$k = 0.6557 \sqrt{\text{secant}\left[\frac{\pi}{2}\left(\frac{D + L}{W - L}\right)\right]}$$

For hole face A: L = 0.048 in. D = 0.190 in. W = 1.00 in. k = 0.6822

For hole face B: L = 0.045 in. D = 0.190 in. W = 1.00 in. k = 0.6813

Figures 4-19 and 4-20 show the results of loading this specimen. It is shown that in both cases the slopes of the K_I curve obtained by caustics were less than the slope of the theoretical line.

An aluminum rivet was installed into the A/D hole. The riveting process produced an epicycloid-shaped zone as shown in Fig. 4-21. The caustic at the crack tip is visible along the cusp axis. The caustic diameter (0.45 in. - photo size) remained constant in the range 0-18 ksi.

Specimen No. 6

Material - 4340V - Normalized to 90 KSI.

Width - 1.00 in.

Thickness - 0.120 in.

Hole Dia - 0.250 in.

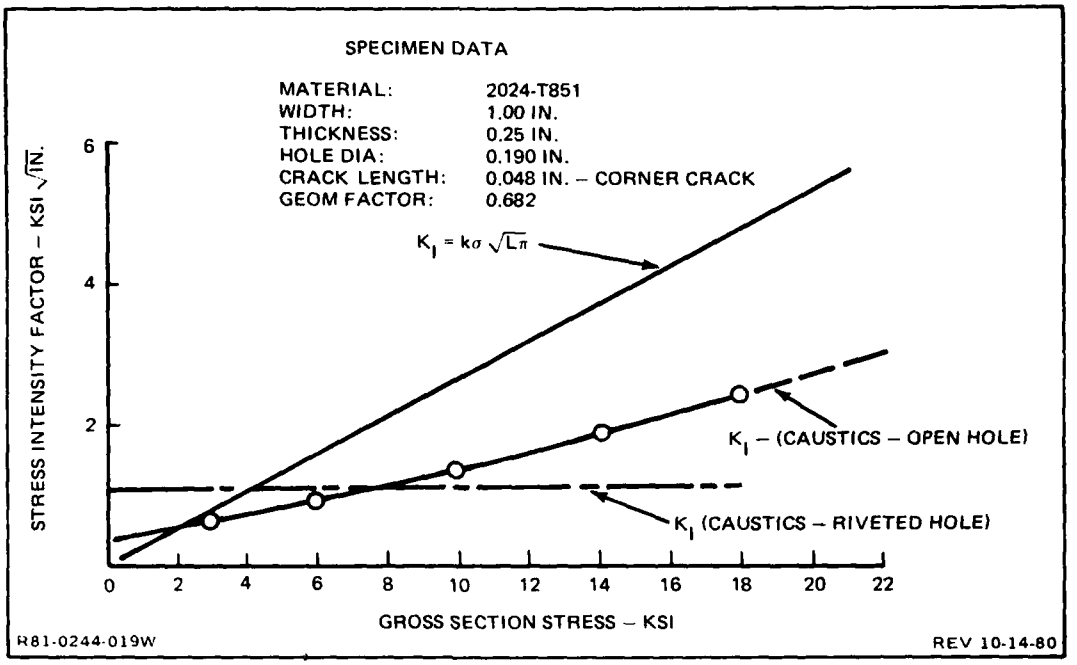

Fig. 4-19 Stress Intensity Factors (ksi $\sqrt{\text{in.}}$), Caustics vs Theory, Specimen 5A

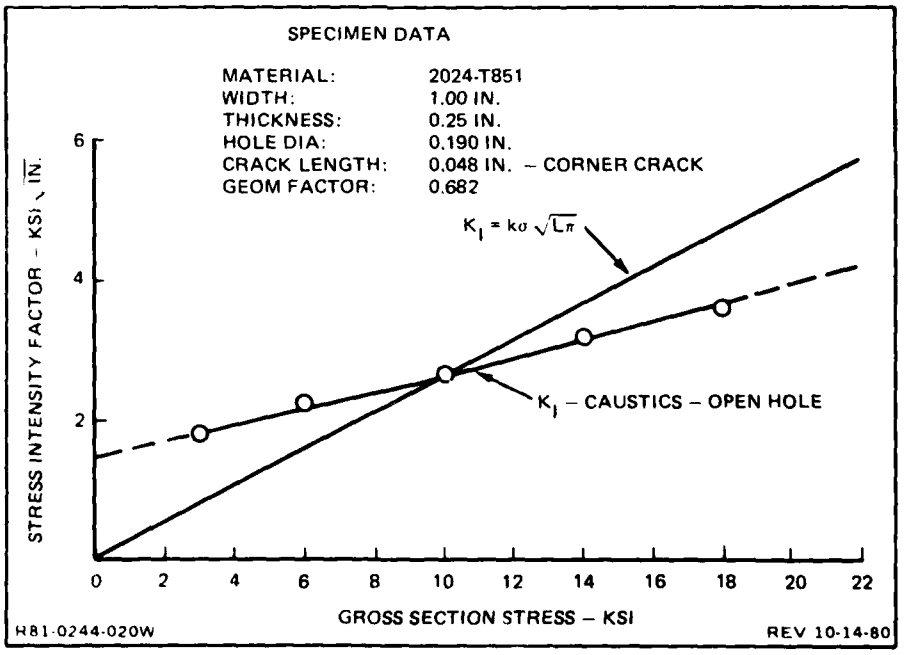

Fig. 4-20 Stress Intensity Factors (ksi $\sqrt{\text{in.}}$), Caustics vs Theory, Specimen 5B

A. CAUSTIC OF RIVETED AREA

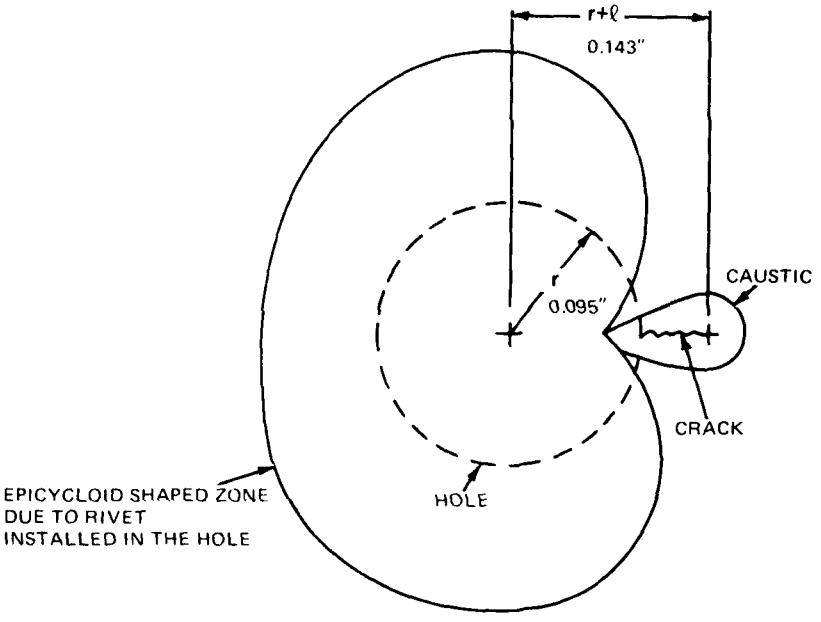

B. EXPLANATORY DIAGRAM OF CAUSTIC SHOWN ABOVE

R81-0244-048W

Fig. 4-21 Caustic of Riveted Area for Specimen No. 5, Hole A/D

This specimen was the first of two steel specimens treated. Crack lengths of 0.028 - 0.047 in. were obtained at the six hole faces. Loading was started at face A, and it was noted that crack tip yielding occurred between 28. - 37.5 ksi. The K_I by caustics was higher than the theoretical line at all points recorded. The data available is plotted in Fig. 4-22. Large residual caustics were observed at the other five hole faces. The K_I range was: 54.9 - 134.1 ksi$\sqrt{in}$.

Steel rivets were driven into all three holes. The heads of the rivets on faces A through C were ground away to improve visibility. However, surface distortion masked all crack and crack tip caustics.

The cracks on the specimen were extended by additional fatigue cycles to determine if the caustics would reappear as follows:

Hole Letter:	A	B	C
Initial Crack Length:	0.042	0.028	0.024
Final Crack Length:	0.042	0.049	0.040

Photographs were taken of the entire zone between the edges of the specimen and the rivet. There were no visible crack or crack tip caustics.

Specimen No. 7

Material - 4340V - Heat treated to 200 ksi

Width - 1.00 in.

Thickness - 0.120 in.

Hole Dia - 0.250 in.

Crack lengths of 0.031 - 0.049 in. were generated in this heat treated steel specimen. The resulting geometry factors (k) were 2.166 to 1.878. Loading was accomplished over a range of 7.5 to 37.5 ksi gross section stress. In all five readable cases, the K_I by caustics was substantially lower than predicted by the theoretical line. Figures 4-23 through 4-27 show these results.

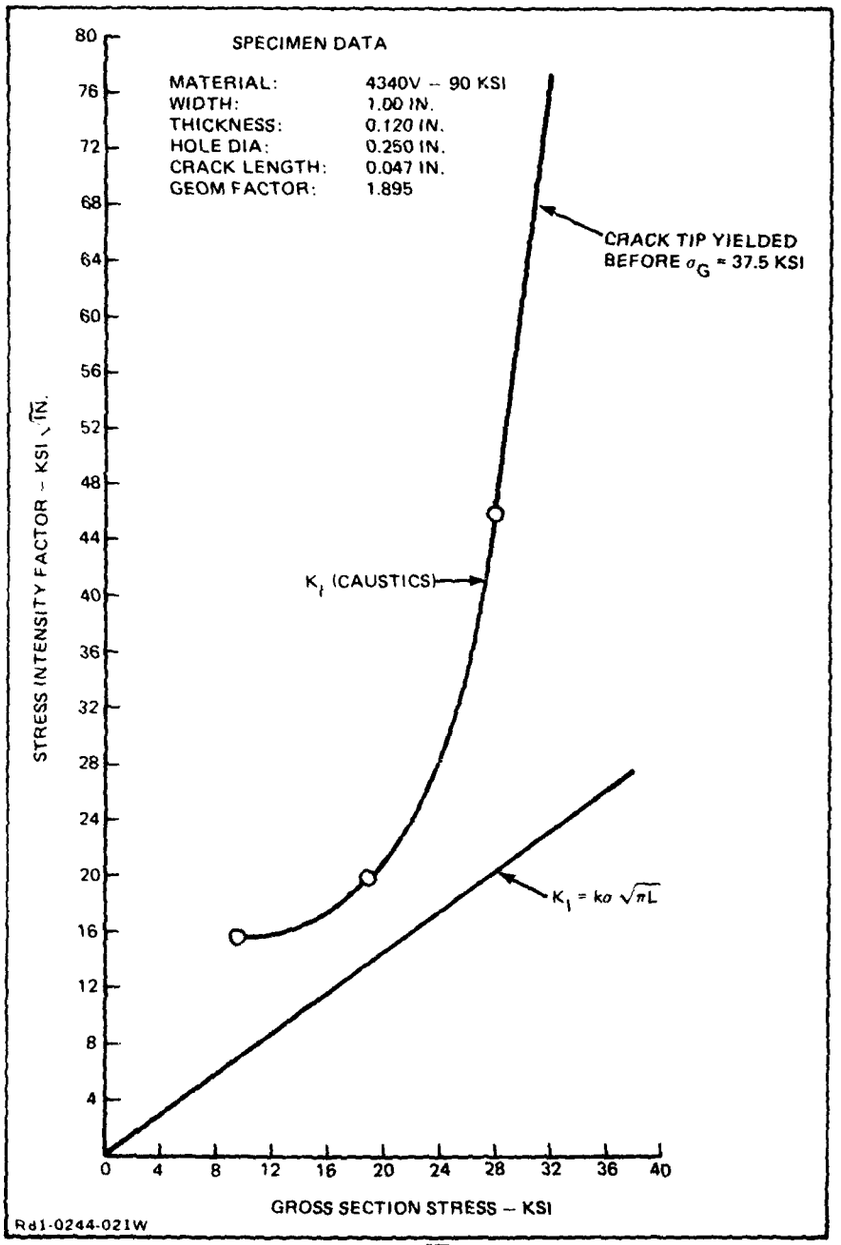

Fig. 4-22 Stress Intensity Factors (ksi $\sqrt{in.}$), Caustics vs Theory, Specimen 6A

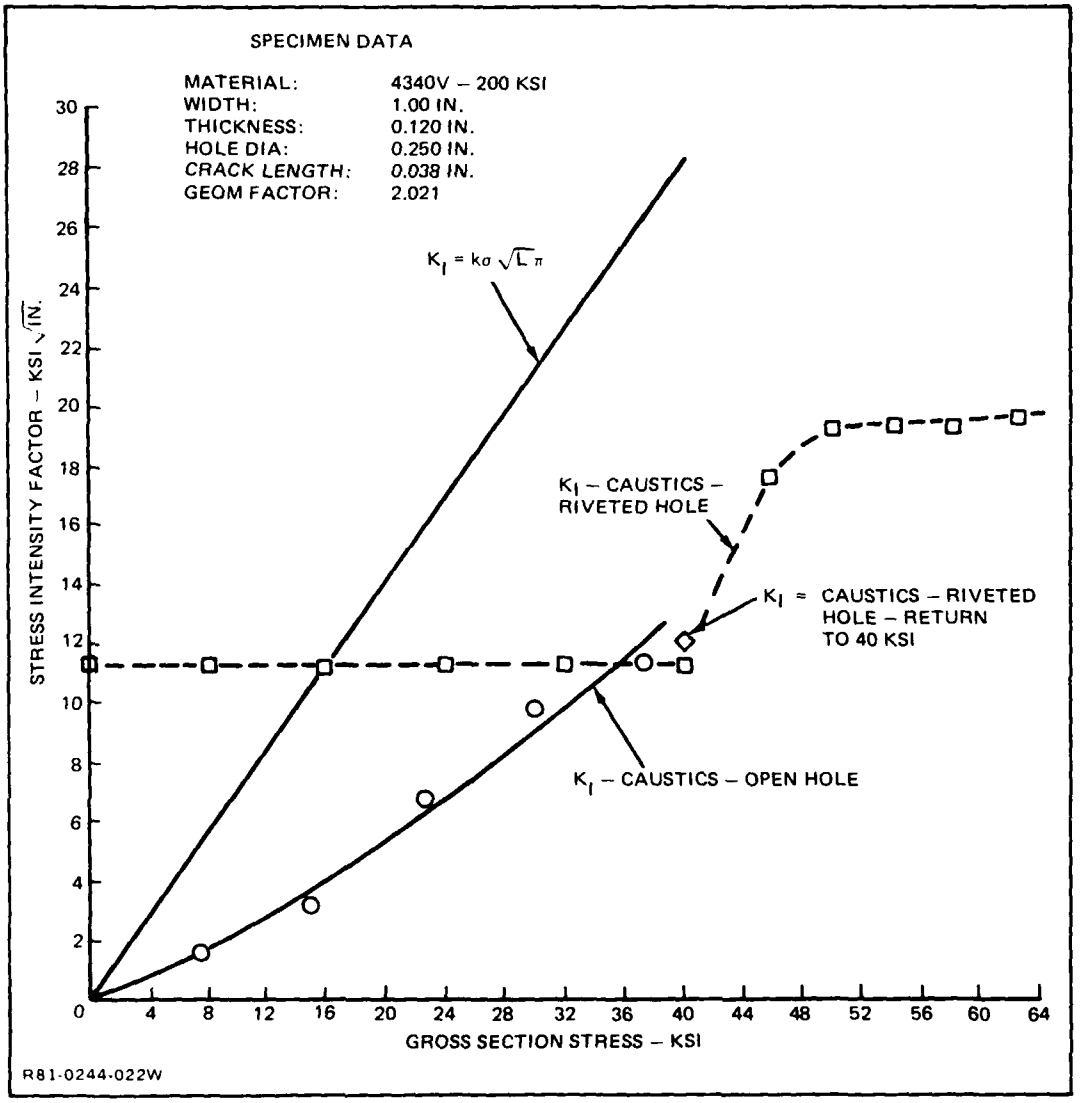

Fig. 4-23 Stress Intensity Factors (ksi $\sqrt{\text{in.}}$), Caustics vs Theory, Specimen 7B

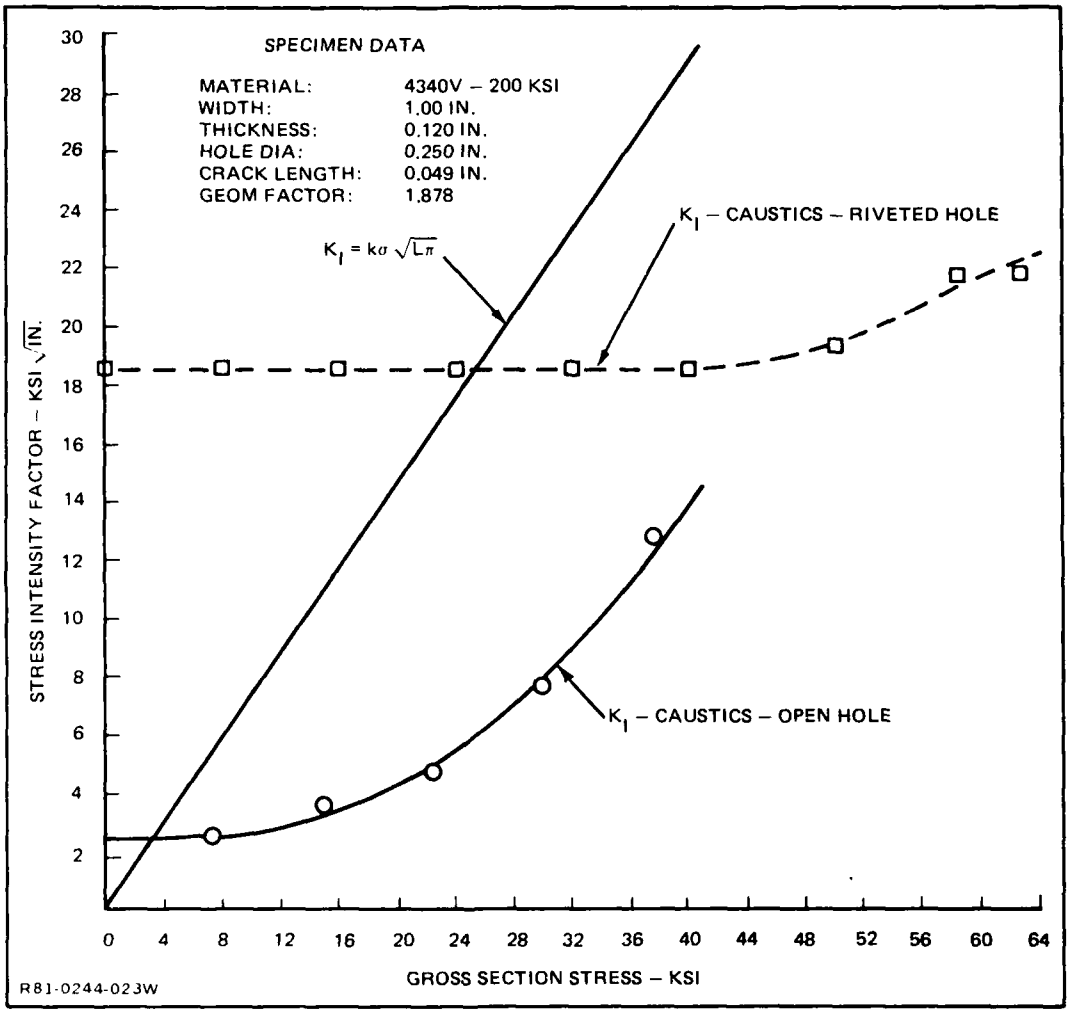

Fig. 4-24 Stress Intensity Factors (ksi $\sqrt{in.}$), Caustics vs Theory, Specimen 7C

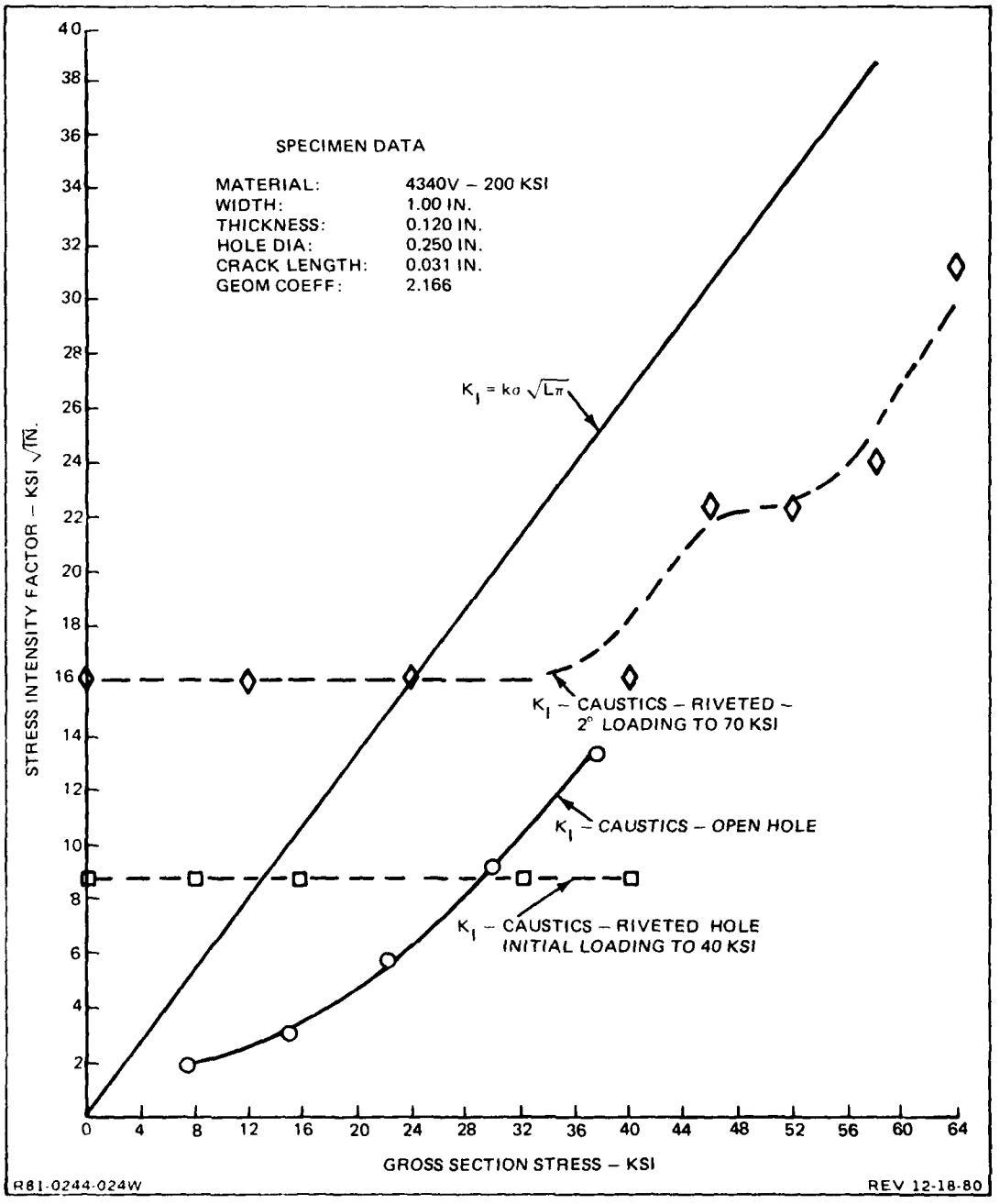

Fig. 4-25 Stress Intensity Factors (ksi $\sqrt{in.}$), Caustics vs Theory, Specimen 7D

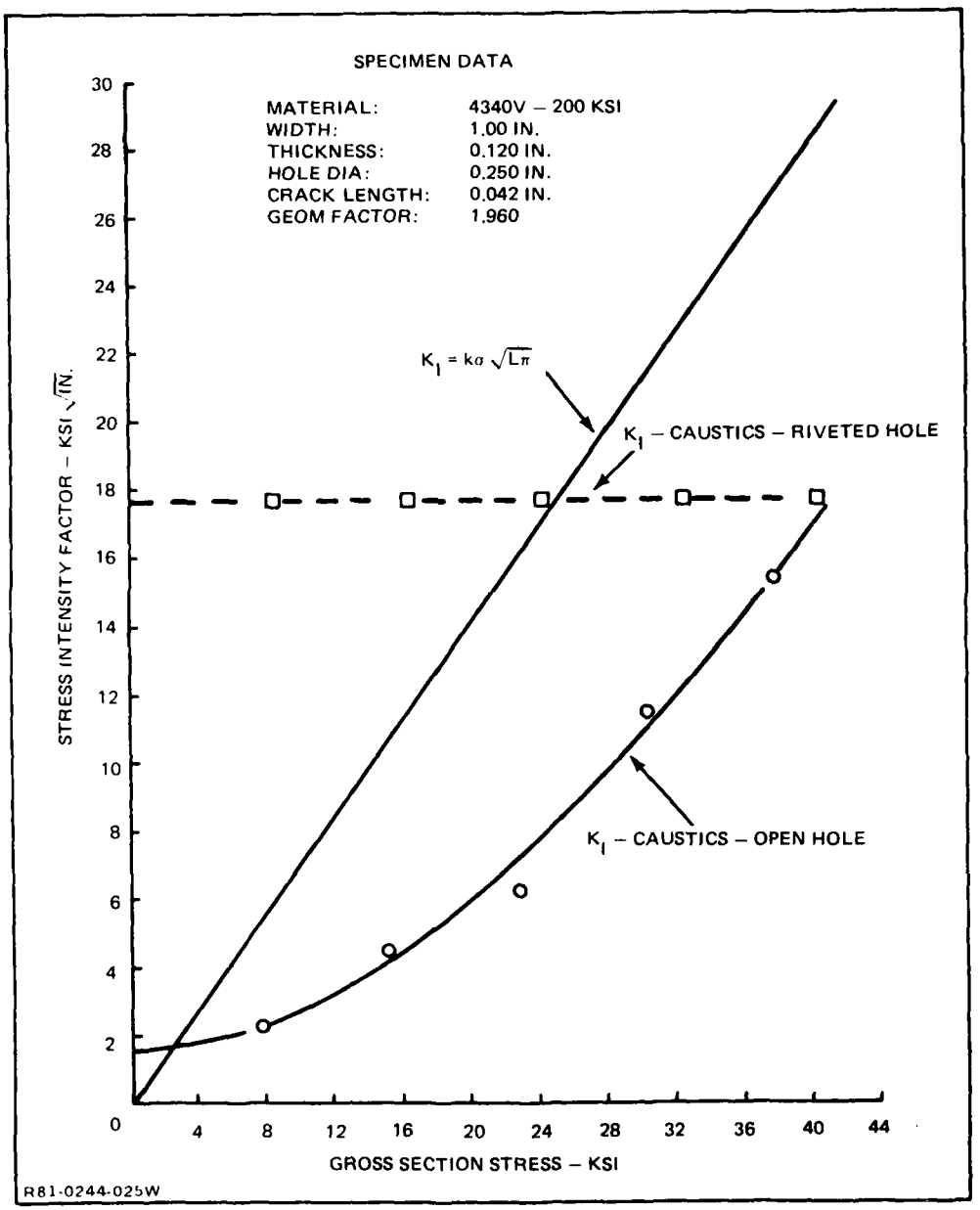

Fig. 4-26 Stress Intensity Factors (ksi $\sqrt{\text{in.}}$), Caustics vs Theory, Specimen 7E

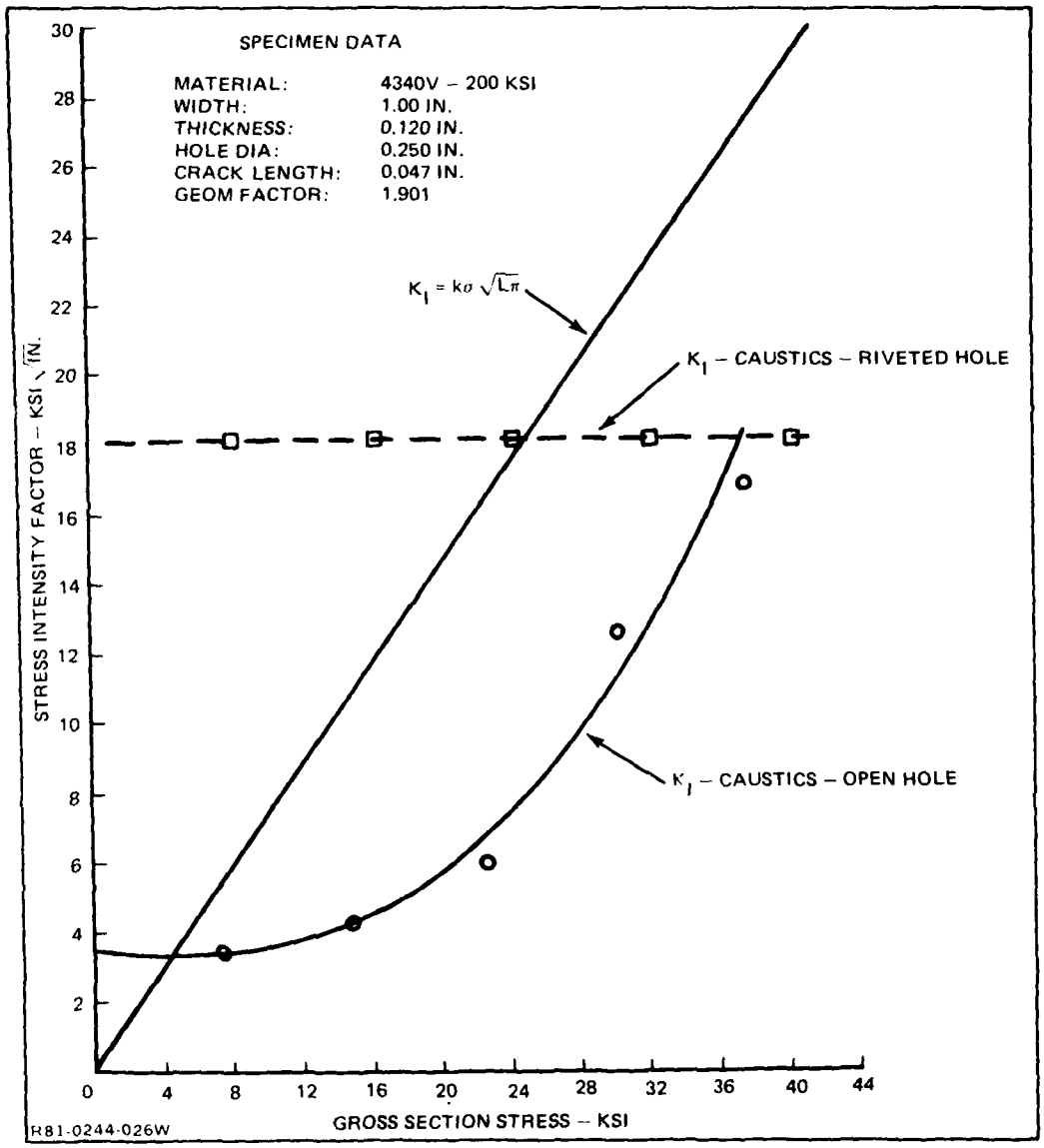

Fig. 4-27 Stress Intensity Factors (ksi $\sqrt{in.}$), Caustics vs Theory, Specimen 7F

Steel rivets were driven into all three holes. The cracks and crack tip caustics were still visible in all five holes of this hardened material. For gross section stresses of 0-40 ksi, the caustic size remained constant in all cases. On two hole faces, B and C, the loading was continued to 70.8 ksi (8500 lbs). For hole face B, the caustic diameter increased sharply between 40-50 ksi, then remained constant through 71 ksi. Hole face C showed a very slow irregular increase in caustic diameter. With the exception of hole face D, all of the holes returned to their initial zero load diameters after loading to 71 ksi. The results of testing on Specimen No. 7 are plotted in Figs. 4-23 through 4-27.

5. DISCUSSION OF RESULTS

The purpose of this report was to carry out a feasibility demonstration of setting up and understanding the method of caustics to determine K_I in situations where the results of the conventional analytical method may not be adequate. We believe that feasibility is clearly demonstrated in the results. Although the basic relationship employed in relating caustics to K_I (Eq (40) of Section 2) requires the value of D to be measured experimentally, the equation itself is based on the theoretical premises, developed by Muskhelishvili and Westergaard and stated by Paris and Sih (Ref 5) and therefore the caustic method is not a purely experimental one. One can say that both equations represent a model of stress and strain at the tip of the crack, with the caustics equation providing a more detailed representation of actual conditions since we measure the local conditions in each individual case. The Paris and Sih equation (actually first derived by Bowie (Ref 6): $K_I = k\sigma\sqrt{L\pi}$, implies, for example, that at $\sigma = 0$, $K_I = 0$. Yet, we know that at any crack tip there is always a residual elastic stress field that assigns K_I a value, even at $\sigma = 0$. The caustics method easily infers this "zero load" condition.

Other difficult conditions exist such that a simple theoretical equation for K_I cannot easily be derived. One such case is the existence of residual compressive stress around the hole. Again, in this case the existence or lack of the caustic can be experimental evidence of the effect of the residual stress field.

The results obtained with the method of caustics also indicate that the opening-mode stress intensity factor K_I is not a linear function of load, as implied by the equation $K_I = k\sigma\sqrt{L\pi}$. We do not have an explanation for this as yet, but we do believe, as stated above, that

the method of caustics represents the behavior of the crack more accurately than the classical theory. The results indicate that there is greater disagreement between the method of caustics and the equation $K_I = k\sigma\sqrt{L\pi}$, for $1.3 < k < 2.00$. This disagreement occurs with small cracks (i.e., 0.005 in. - 0.050 in.) and although it is not yet proven, we believe that it is due to the biaxial stress field near the hole, which only the caustics method takes into account.

The tests that were carried out with the steel specimens (6 and 7) showed that for the same load, the caustics of the normalized (softer) specimen were considerably larger than the corresponding caustics of the hardened specimen. This behavior was expected from physical reasoning, since a lower yield stress will allow a more extensive deformation by plastic deformation prior to parting at the crack tip. Since Eq (40) of Section 2 was derived for purely elastic cases, it cannot show this behavior, nor can the Paris and Sih equation. The sudden increase in the caustic size, however, can be a useful indication of incipient plastic deformation, an indication not easily displayed by analytical models.

With the above principles in mind, we proceed to discuss the results presented in the preceeding section in more detail. In several of these cases, no caustic appeared. Because of the newness of the technique, it is usually not possible to be sure what the reason may be for lack of a caustic in a given case. It may indicate that K_I has gone to zero because of the beneficial effects of residual stresses. It may be that the caustic has been destroyed by surface distortions induced by the riveting process. The appearance of an enhanced caustic after riveting is currently interpreted to imply that the crack tip is in the region of residual tension stress, where crack propagation would be enhanced by the residual stress field. These points should be kept in mind in the following discussion.

In total, 25 open pre-cracked hole faces were analyzed without rivets installed (open-hole case). A review of the plots (Figs. 4-2 through 4-27) shows that in only one of these cases (6A) was the K_I

value obtained by caustics substantially and consistently higher than the theoretical line. This was the case for annealed 4340 steel, and is explained by excessive plastic deformation, as discussed above. In general then, the test data tend toward the conclusion that for meaningful fatigue stress levels (i.e., for gross section stresses greater than 6-8 ksi) the K_I value obtained by caustics is less than or equal to the theoretical line. With some exceptions (3F, 4B, 4C, and 4D) if geometry factor is greater than 1.3, the K_I inferred by caustics is substantially less than the theoretical line. For geometry factors less than 1.3 the K_I obtained by caustics is approximately equal to that obtained from the theoretical line.

When steel interference-fit rivets were installed in the aluminum or soft steel specimens significant surface distortion occurred. This distortion is a natural result of the plastic deformation that is the goal of stress wave riveting. In only three cases (3B, 3F, and 4C) were residual caustics visible. These cases produced large static residual K_I values, which did not change with applied load through gross section stresses equal to 18 ksi. The crack lengths for these cases (0.134, 0.168, and 0.060 in., respectively) place the crack tip outside the region of compressive residual stress into the zone of hoop tension. A large static residual K_I would be the expected result, and cracks of these lengths would be accelerated by riveting if our interpretation is correct. The absence of a caustic in the balance of the cases implies that compressive residual stresses work to reduce or eliminate stress intensity factors, thus working to arrest crack growth.

When steel interference-fit rivets were installed into the hardened steel specimen (7B-7F) static residual caustics were observed to exist at all five readable hole faces. These caustics remained constant in size through applied loads producing gross section stresses of 40 ksi. When the loading was continued beyond 40 ksi to 71 ksi, the caustics were observed to grow slowly and irregularly. It was also noted that with one exception (7D) all of the caustics returned to their initial zero load diameters after being loaded to 71 ksi gross section stress. The caustics at hole "D" enlarged from a K_I value of 8.74 ksi $\sqrt{\text{in.}}$ to

16.18 ksi in. at zero load. As before, it remained constant through 40 ksi, then increased sharply to a K_I = 35.54 ksi $\sqrt{in.}$ at 70 ksi gross section stress. This interesting behavior is deserving of additional study.

It should be pointed out that clarity of the caustic epicycloid, and the ability to accurately measure it, is directly related to the flatness of the surface. Due to the exploratory nature of this first test series, all of the specimens were polished by hand. Better polishing methods (i.e., machine lapping) should be used for any subsequent work in this field. It is possible that some or all of the anomalies seen in these tests are the result of distortion of the caustic epicycloid by localized surface irregularities.

Specimen 7D has been chosen to illustrate the caustics method, since it represents the clearest of the caustic photographs obtained, and is representative of the test procedure which was followed. Figure 5-1 shows the caustics for the cracked open hole case. Figure 5-2 shows the same hole with an interference fit fastener installed during the loading series in which all the holes were loaded to a maximum of 40 ksi. Finally, Fig. 5-3 shows the same hole during a later series of loads in which the hole had already been loaded to a maximum of 71 ksi. These three pictures are of caustics for which K_I values are plotted in Fig. 4-25. This is a case for which riveting had little beneficial effect in reducing K_I, probably because the high yield stress prevented significant plastic deformation in the surrounding steel, so the beneficial residual compressive stress did not have much effect. In those cases where the benefits of residual stress were great, the caustics are either non-existent or much less detectable than in specimen 7D.

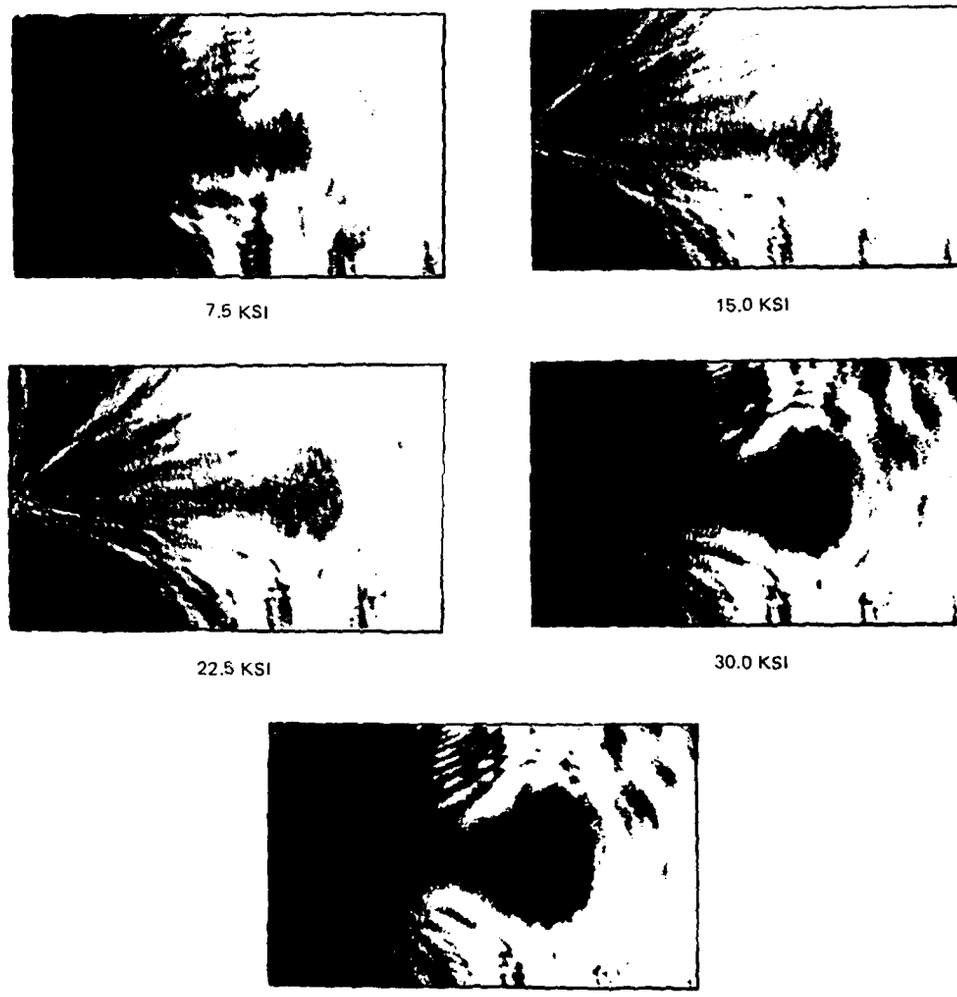

Fig. 5-1 Specimen 7D – Open Hole

R81-0244-030-V

Fig. 5-2 Specimen 7D – with Rivet – Initial Loading to 40 ksi

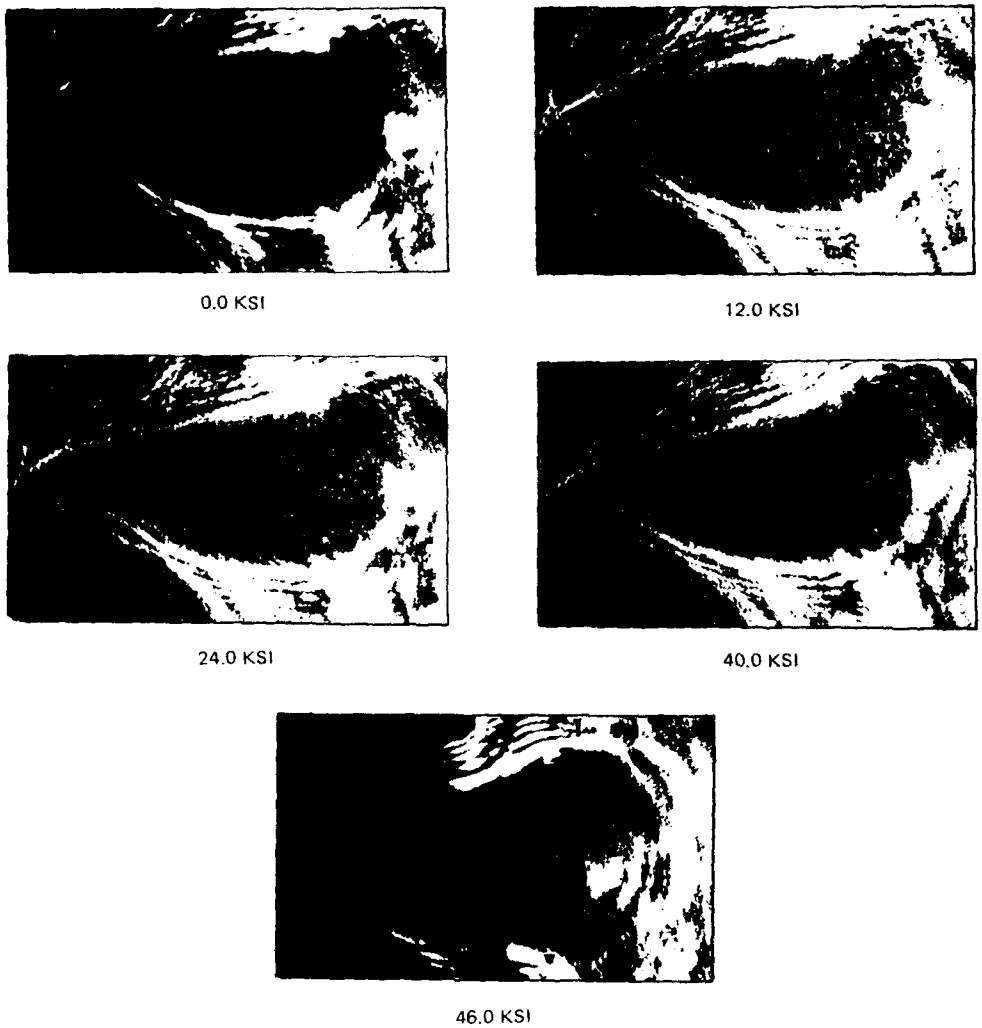

R81-0244-031W(1 2)

Fig. 5-3 Specimen 7D – with Rivet – Later Loading to 70 ksi (Sheet 1 of 2)

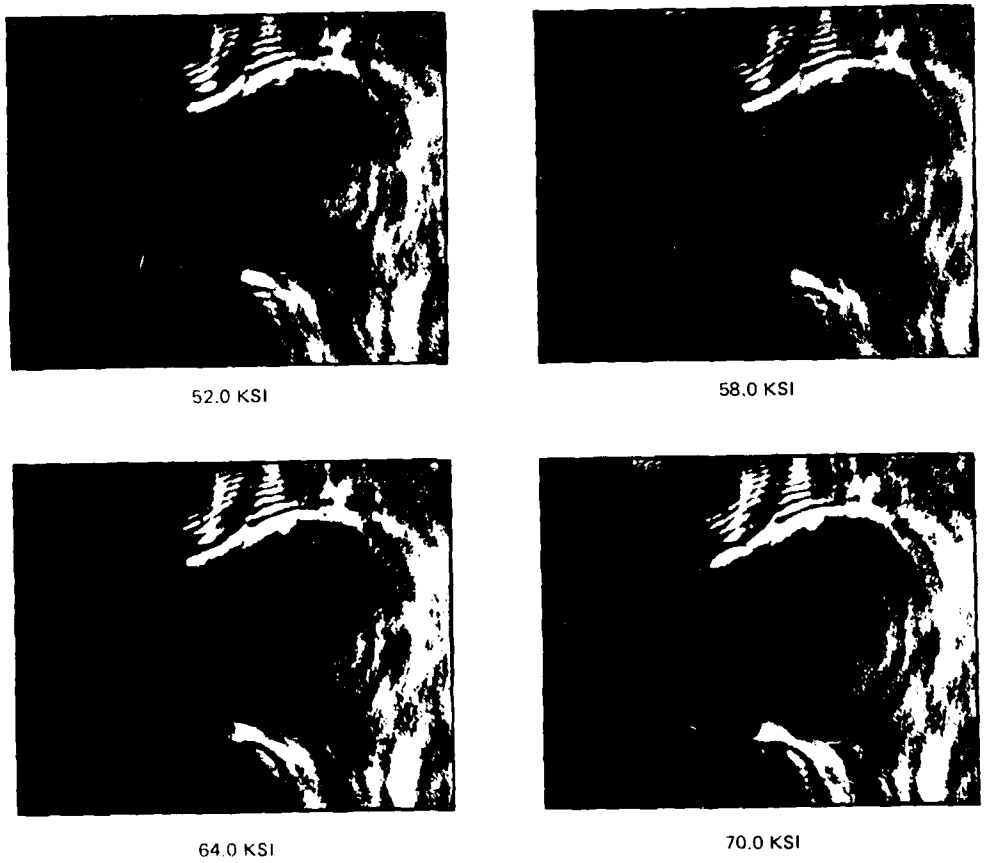

R81-0244-031WI(2-2)

Fig. 5-3 Specimen 7[illegible] – with Rivet – Later Loading to 70 ksi (Sheet 2 of 2)

6. CONCLUSIONS

The method of caustics promises to be a very useful tool for the investigation of stress intensities in localized-stress regions such as those near crack tips. As a complement to purely analytical treatment of such regions, it provides direct measurements of surface distortions in such regions, giving insight into such factors as the influence of imposed residual stress, the natural residual stress field induced as the crack forms, the effects of hardness, and perhaps other factors not yet discovered.

This preliminary investigation of the use of caustics indicates that stress intensity factors follow the general characteristics of theoretical predictions, except in certain special situations. At low stress levels, the caustics results indicate a zero-load value of K_I that is substantial, and not predicted by the classical (elastic) theory. At values of the geometric factor greater than 1.3, the caustics values are substantially below the theoretical predictions. As loading begins to approach the yield stress of the material, there is a tendency for the caustic values to increase relative to the theoretical predictions.

When plastic deformation of the region surrounding the precracked hole is introduced by installation of a stress wave driven rivet, the caustics disappear if the tip of the crack lies within the region of residual compressive stress; at least until the loading is increased to high values. In a few cases when the crack tip lies outside the compressive residual region, the no-load K_I indicated by caustics is substantially increased. Preliminary indications from these results are that stress wave installed rivets can arrest cracks up to a critical length that depends on the rivet installation parameters, at least for loading less than a particular level.

7. REFERENCES

1. Leftheris, B.P., Eidinoff, H. and Hooson, R.E., "Evaluation of Dynamically Riveted Joints," Report No. NADC-77202-30, July 1979; Grumman Research Department Report RE-587.

2. Leftheris, B.P., "Advantages of Residual Stresses in Dynamically Rivet Joints," Grumman Research Department Report RE-552, Feb. 1978.

3. Theocaris, P.S., "Complex Stress-Intensity Factors at Bifurcated Cracks," J. Mech. Solids, Vol. 20, pp. 265-279, 1972.

4. Theocaris, P.S., "Local Yielding Around a Crack Tip in Plexiglass," J. of Appl. Mech., June 1970.

5. Paris, P.C. and Sih, G.C., "Stress Analysis of Cracks," ASTM Special Tec. Publ. 381, 1964.

6. Bowie, O.L., "Analysis of an Infinite Plate Containing Radial Cracks Originating from the Boundary of an Internal Circular Hole," J. of Math. and Phys., Vol. 35, 1956.

APPENDIX

FRACTURE MECHANICS BACKGROUND

Structural materials of crystalline structure usually fracture at strengths well below their theoretical strength levels. Such premature failures are caused by the many structural imperfections which, when combined with oscillating tension loads, initiate cracks that result in fractures.

The contemporary approach to structural design accepts material imperfections as facts of life. To accommodate their presence and avoid their catastrophic effects, designers and stress analysts use various theoretical and empirical techniques.

Fracture analysis identifies three types of cracks as shown below:

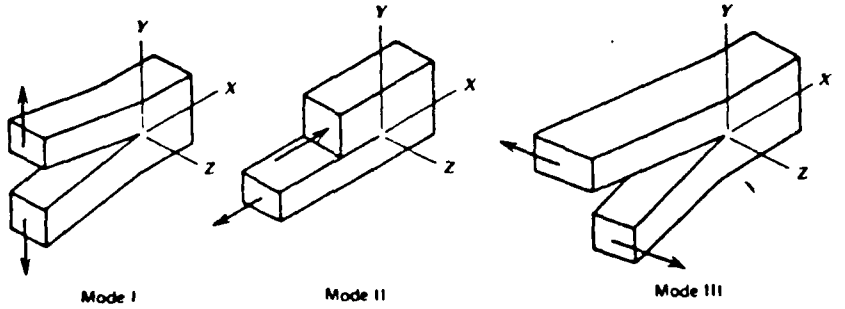

Our applications relate to the cracks emanating from a hole, or Mode I crack surface displacement, as shown in Fig. A-1.

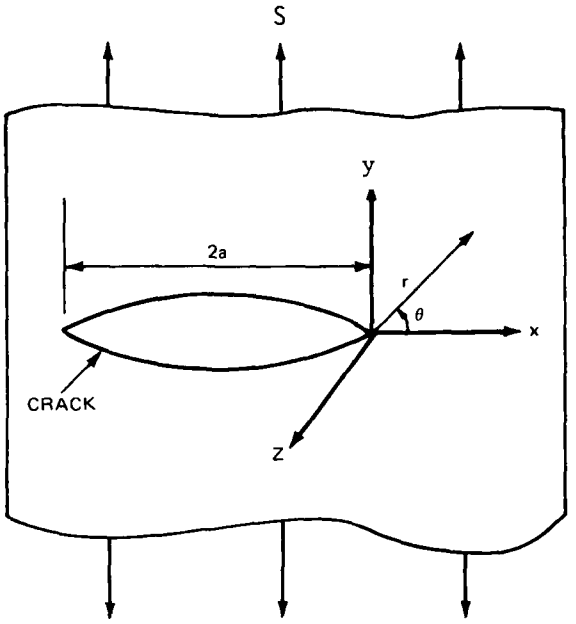

WHERE S = REMOTELY APPLIED TENSION.

Fig. A-1 Specimen Containing Mode I Crack

where S = remotely applied tension.

Dimensional analysis and geometrical considerations show that the stress intensity factor for Mode I is given by

$$K_I = S\sqrt{\pi a}$$

Following Ref. 5, the elastic stress distribution at the crack tip for Mode I is given by the following equations (see Fig. A-1.)

$$\sigma_x = \frac{K_I}{\sqrt{2\pi r}} \cos\frac{\theta}{2}\left[1 - \sin\frac{\theta}{2}\sin\frac{3\theta}{2}\right] \qquad \text{(A-1)}$$

$$\sigma_y = \frac{K_I}{\sqrt{2\pi r}} \cos\frac{\theta}{2}\left[1 + \sin\frac{\theta}{2}\sin\frac{3\theta}{2}\right] \qquad \text{(A-2)}$$

$$\tau_{xy} = \frac{K_I}{\sqrt{2\pi r}} \sin\frac{\theta}{2}\cos\frac{\theta}{2}\cos\frac{3\theta}{2} \qquad \text{(A-3)}$$

$$\tau_{xz} = \tau_{yz} = 0$$

and $\sigma_Z = \begin{cases} = 0 \text{ plane stress} \\ \nu\ (\sigma_x + \sigma_y) \text{ plane strain} \end{cases}$

where σ_x, σ_y, σ_z are stresses in the x, y, Z directions and τ_{xy}, τ_{xz}, τ_{yz} are shear stresses.

and K_I = the stress intensity factor.

The equations above clearly show that for any radius r, the intensity of the stresses depends on the value of K_I. For example, taking an element at $\theta = 0$ will result in $\sigma_x = \sigma_y = K_I / \sqrt{2\pi r}$.
The crack distribution is as shown below.

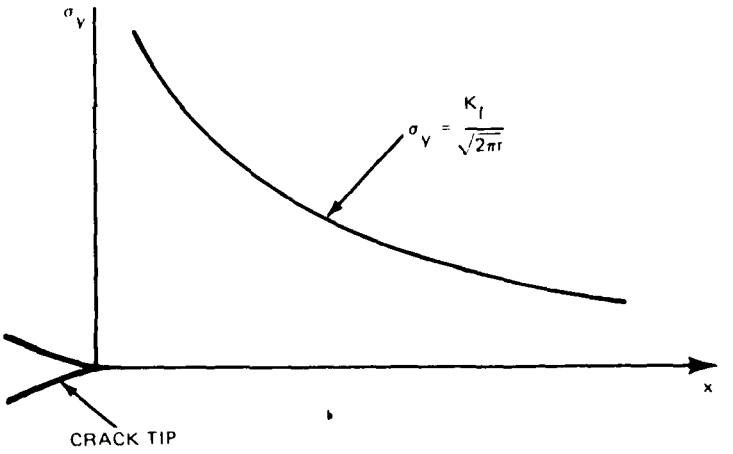

The meaning of K_I is closely related to that of K_T, the stress concentration factor. K_I and K_T, however, are not interchangeable. For example, the hoop stress distribution of a uniaxially loaded specimen with a hole in its center is shown below:

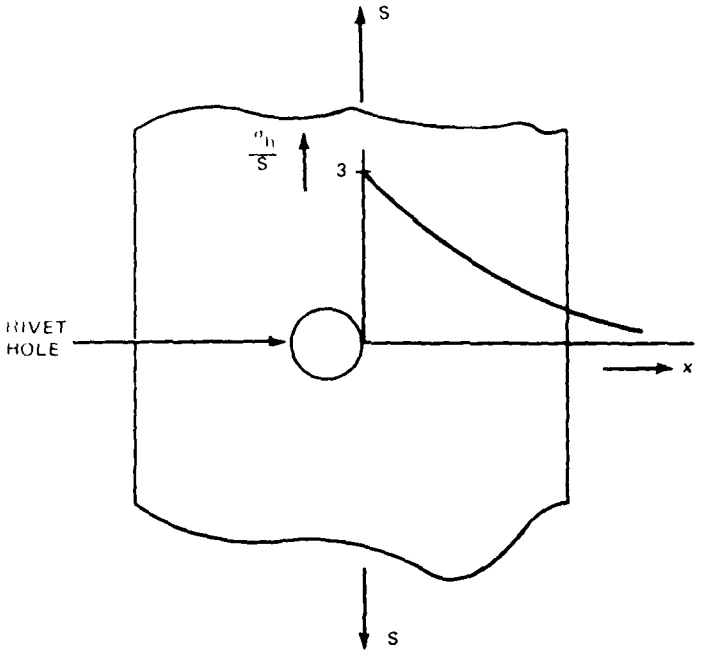

WHERE

σ_h = HOOP STRESS NEAR HOLE

S = REMOTELY APPLIED TENSION

$K_T = \frac{\sigma_h}{S}$ AT

x = 0, OR $K_T = 3$

In crack problems with the crack embedded in an infinite plate at an angle β with the axis of loading, we can use the complex stress function $\phi(\zeta)$ for the region close to the crack tip. From Ref 5, the stress function is given by

$$\phi(\zeta) = \frac{K^*}{2(2\pi\zeta)^{1/2}} \qquad \text{(A-4)}$$

where $K^* = K_I - iK_{II}$

K_I = stress intensity factor for the opening mode

K_{II} = Stress intensity factor for the sliding mode

$\zeta = re^{i\theta}$.


DAT
FILM